Terminal Differentiation, Advanced Organotypic Maturation, and Modeling of Hypertrophic Growth in Engineered Heart Tissue

Malte Tiburcy, Michael Didié, Oliver Boy, Peter Christalla, Stephan Döker, Hiroshi Naito, Bijoy Chandapillai Karikkineth, Ali El-Armouche, Michael Grimm, Monika Nose, Thomas Eschenhagen, Anke Zieseniss, Doerthe M. Katschinksi, Nazha Hamdani, Wolfgang A. Linke, Xiaoke Yin, Manuel Mayr and Wolfram-Hubertus Zimmermann

Circulation Research 2011, 109:1105-1114: originally published online September 15, 2011
doi: 10.1161/CIRCRESAHA.111.251843
Circulation Research is published by the American Heart Association. 7272 Greenville Avenue, Dallas, TX 72514
 Print ISSN: 0009-7330. Online ISSN: 1524-4571

Terminal Differentiation, Advanced Organotypic Maturation, and Modeling of Hypertrophic Growth in Engineered Heart Tissue

Malte Tiburcy,* Michael Didié,* Oliver Boy, Peter Christalla, Stephan Döker, Hiroshi Naito, Bijoy Chandapillai Karikkineth, Ali El-Armouche, Michael Grimm, Monika Nose, Thomas Eschenhagen, Anke Zieseniss, Doerthe M. Katschinksi, Nazha Hamdani, Wolfgang A. Linke, Xiaoke Yin, Manuel Mayr, Wolfram-Hubertus Zimmermann

Rationale: **Cardiac tissue engineering should provide "realistic" in vitro heart muscle models and surrogate tissue for myocardial repair. For either application, engineered myocardium should display features of native myocardium, including terminal differentiation, organotypic maturation, and hypertrophic growth.**

Objective: **To test the hypothesis that 3D-engineered heart tissue (EHT) culture supports (1) terminal differentiation as well as (2) organotypic assembly and maturation of immature cardiomyocytes, and (3) constitutes a methodological platform to investigate mechanisms underlying hypertrophic growth.**

Methods and Results: **We generated EHTs from neonatal rat cardiomyocytes and compared morphological and molecular properties of EHT and native myocardium from fetal, neonatal, and adult rats. We made the following key observations: cardiomyocytes in EHT (1) gained a high level of binucleation in the absence of notable cytokinesis, (2) regained a rod-shape and anisotropic sarcomere organization, (3) demonstrated a fetal-to-adult gene expression pattern, and (4) responded to distinct hypertrophic stimuli with concentric or eccentric hypertrophy and reexpression of fetal genes. The process of terminal differentiation and maturation (culture days 7–12) was preceded by a tissue consolidation phase (culture days 0–7) with substantial cardiomyocyte apoptosis and dynamic extracellular matrix restructuring.**

Conclusions: **This study documents the propensity of immature cardiomyocytes to terminally differentiate and mature in EHT in a remarkably organotypic manner. It moreover provides the rationale for the utility of the EHT technology as a methodological bridge between 2D cell culture and animal models. (*Circ Res*. 2011;109:1105-1114.)**

Key Words: cardiac myocytes ■ caspase activation ■ extracellular matrix ■ maturation ■ hypertrophy ■ sarcomere ■ tissue engineering

Different myocardial tissue engineering formats have been developed throughout the past decade.[1] However, a low degree of cell maturation remains a key caveat in cardiac muscle engineering. A detailed understanding of "developmental" processes in tissue engineered myocardium probably is essential to guide tissue formation and maturation in vitro and to enhance the applicability of tissue engineered myocardium in substance screening, target validation, and tissue repair.

Normal heart muscle growth encompasses processes of terminal differentiation and maturation by hypertrophic growth, leading to the formation of binucleated and rod-shaped myocytes.[2] Physiological maturation entails a characteristic shift in gene expression, including a reduction of transcripts encoding for fetal isoforms of myofibrillar proteins while the proportion of adult isoforms increases.[3] Terminal differentiation, for example, withdrawal from the cell cycle, is another hallmark of advanced maturation already reached very early during development.[4]

Cardiomyocyte monolayer cultures show neither the distinct morphological (rod-shaped) nor the molecular (adult gene expression program) make-up of mature myocytes,[5–7]

Original received July 5, 2011; revision received August 22, 2011; accepted September 7, 2011. In August 2011, the average time from submission to first decision for all original research papers submitted to *Circulation Research* was 13.5 days.

From the Department of Pharmacology, Georg-August-University Goettingen, Germany (M.T., M.D., O.B., P.C., S.D., H.N., B.C.K., A.E.-A., W.-H.Z.); Institute of Experimental and Clinical Pharmacology, University Medical Center Hamburg-Eppendorf, Germany (M.G., M.N., T.E.); the Department of Cardiovascular Physiology, Georg-August-University Goettingen, Germany (A.Z., D.M.K.); the Department of Cardiovascular Physiology, Institute of Physiology, Ruhr University Bochum, Germany (N.H., W.A.L.); and King's BHF Centre, King's College, University of London, United Kingdom (X.Y., M.M.).

*These authors contributed equally to the study.

Correspondence to Wolfram-Hubertus Zimmermann, MD, Department of Pharmacology, Georg-August-University Goettingen, Robert-Koch-Str 40, 37075 Goettingen, Germany. E-mail w.zimmmermann@med.uni-goettingen.de

Circulation Research **is available at http://circres.ahajournals.org** **DOI: 10.1161/CIRCRESAHA.111.251843**

Non-standard Abbreviations and Acronyms	
ANP	atrial natriuretic peptide
DAPI	4′,6-diamidino-2-phenylindole
ECM	extracellular matrix
EHT	engineered heart tissue
MHC	myosin heavy chain
MLC2v	myosin light chain, ventricular isoform
MMP	matrix metalloprotease
PHD	prolyl-4-hydroxylase domain enzyme
TIMP	tissue inhibitor of MMP
VEGF	vascular endothelial growth factor

probably as a consequence of the lack of a 3D growth environment and inappropriate biomechanical loading. Despite some evidence for advanced maturation in 3D tissue engineering models, it remains unclear whether cardiomyocytes in tissue engineered myocardium can, and if so to what extent, develop "physiologically" ex vivo.[8,9]

Three fundamentally different myocardial tissue engineering concepts are presently explored: (1) the classic approach involves cell seeding on preformed scaffold material[10–14]; (2) an alternative strategy is based on stacking cell sheets to generate multilayered muscle constructs[15]; (3) we have developed another method, taking advantage of the inherent capacity of immature cardiomyocytes to reassemble into spontaneously beating tissue if maintained at high density in a spatially defined culture environment under defined load.[9,16,17] This cell entrapment method was further refined yielding engineered heart tissues (EHTs) with functional properties of native myocardium.[9]

In the present study, we demonstrate that EHT cultures can support terminal differentiation and tissue-like cardiomyocyte maturation. This finding is underscored by the similarity of morphological and molecular features of EHT- and postnatal heart-derived cardiomyocytes. Interestingly, the process of cardiomyocyte maturation and EHT-development showed 2 distinct phases: (1) a consolidation phase during culture days 0–7 with high levels of apoptotic cell death as well as extracellular matrix (ECM) degradation and (2) a maturation phase during culture days 7–12 with myocyte binucleation, formation of anisotropically organized sarcomeres in preferentially rod-shaped cardiomyocytes, a shift from fetal-skeletal to adult-cardiac actin transcript expression, and ECM build-up. Exposure to different hypertrophic stimuli during the maturation phase elicited distinct hypertrophic phenotypes, that is, concentric or eccentric hypertrophy.

Methods

EHT Construction

EHTs were prepared from collagen type I, Matrigel, as well as neonatal rat heart cells (2.5×10^6) and cultured for 12 days.[9]

^{3}H-Thymidine Incorporation

EHTs were labeled with 1 μCi/mL ^{3}H-thymidine for 6 hours on the indicated culture days. DNA was prepared using standard procedures and subjected to liquid scintillation counting.

Cell Isolation

EHTs or hearts were digested with Liberase Blendzyme III in the presence of 30 mmol/L 2,3-butanedione monoxime at 37°C to prepare cardiomyocytes for morphological assessment by confocal laser scanning microscopy and flow cytometry.

One-Dimensional Electrophoresis and Immunoblotting

EHT protein was separated by SDS-PAGE. For detection of myosin heavy chain (MHC), isoforms gels were stained overnight with SYPRO Ruby. Blots were probed with monoclonal antibodies directed against indicated proteins and developed with ECL-plus.

Two-Dimensional Electrophoresis and Nanoflow Liquid Chromatography Tandem Mass Spectrometry

Protein extracts were separated by 2D electrophoresis. Protein spots were excised and enzymatically degraded. Peptides were separated by a nanoflow HPLC system on a reverse-phase column and applied to an LTQ ion-trap mass spectrometer.

^{3}H-Phenylalanine and ^{3}H-Proline Incorporation

EHTs were labeled with 1 μCi/mL ^{3}H-phenylalanine or ^{3}H-proline as indicated. Protein was precipitated in 10% ice-cold trichloroacetic acid at 4°C overnight and subjected to liquid scintillation counting.

^{35}S-Cysteine/-Methionine Incorporation and Autoradiography

EHTs were labeled with 100 μCi/mL ^{35}S-cysteine/-methionine for 18 hours on the indicated culture days and proteins were separated by SDS-PAGE. Gels were stained with Coomassie blue, immersed in Amplify Fluorographic solution (Amersham Biosciences), vacuum dried, and subjected to autoradiography.

An expanded Methods section can be found online at http://circres.ahajournals.org.

Results

Construction of Spontaneously Contracting EHT

We generated spontaneously contracting EHTs from an initially liquid reconstitution mixture composed of enzymatically dispersed neonatal rat heart cells, collagen type I, and basement membrane proteins (Matrigel).[9] Cell clusters within condensing EHTs started to beat within 2–3 culture days (Online Video I). On culture day 7, all EHTs contracted spontaneously and in unison (Online Video II). After 12 culture days, EHTs demonstrated a solid composition and vigorous contractions (Online Video III).

Hypertrophic Growth of Cardiomyocytes in EHT

The changes in EHT morphology and function prompted us to assess indices of cell proliferation and hypertrophy. We observed a marked reduction in cell number to 30% of the input cells between EHT culture day 0 (day of EHT construction) and day 12 (2.5×10^6 versus $0.8\pm0.03\times10^6$ cells/EHT; n=10; Figure 1A). Despite the cell loss, DNA content decreased only by 42% (45±3 versus 26±1 μg/EHT; n=17–20; Figure 1B), implying a relative increase of DNA content per cell (≈18 versus ≈32 pg DNA/cell on culture days 0 and 12, respectively). Further analysis of cardiomyocyte (α-actinin–positive; Online Figure I, A) and fibroblast (vimentin-positive; Online Figure I, B) quantity indicated that the initial cell loss was mainly the consequence of high cardiomyocyte loss while fibroblast content remained stable

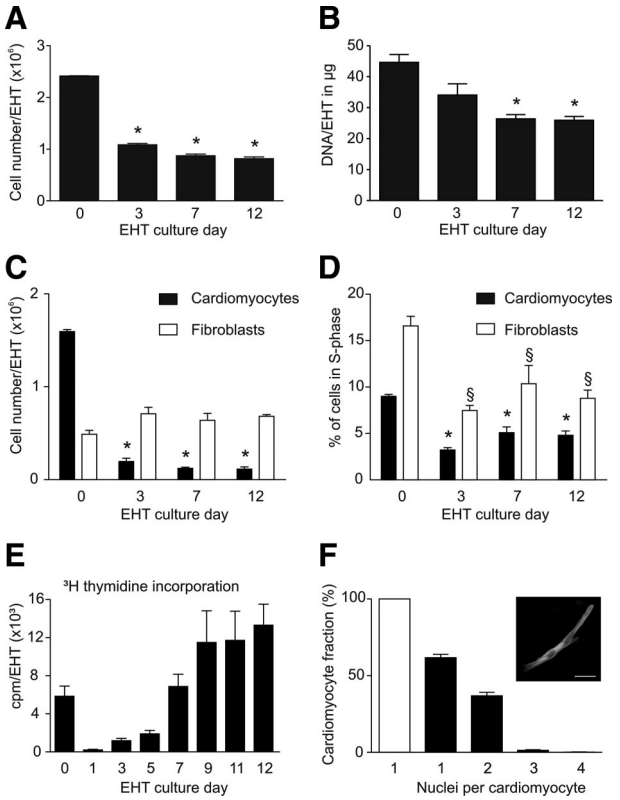

Figure 1. Cell loss and DNA synthesis during EHT culture. **A**, Cell number at the time of EHT casting (culture day 0) and on subsequent culture days 3, 7, and 12 (n=10/time point). **B**, DNA content in EHTs on culture days 0 (n=18), 3 (n=20), 7 (n=17), and 12 (n=20). **C**, Number of cardiomyocytes (actinin-positive cells) and fibroblasts (vimentin-positive cells) at the time of EHT casting (culture day 0, n=8) and on subsequent culture days 3 (n=4), 7 (n=6), and 12 (n=4), assessed by flow cytometry after enzymatic dispersion of EHTs. **D**, DNA synthesis (S-phase) in cardiomyocytes and fibroblasts in EHT on culture days 0 (n=6), 3 (n=4), 7 (n=6), and 12 (n=4), assessed by flow cytometry in DAPI-stained actinin- and vimentin-positive cells. **E**, ^{3}H-thymidine incorporation in EHTs on culture days 0, 1, 3, 5, 7, 9, 11, and 12 (n=9/time point). **F**, Number of nuclei in neonatal rat heart–derived (postnatal days 1–3, n=60; **white bar**) and EHT-derived myocytes on culture day 12 (**black bars**; n=4 EHTs, 30–40 cells each); **inset**: example of a binucleated cardiomyocyte: bar: 10 μm. *$P<0.05$ versus day 0 (**A** through **C**); *$P<0.05$ versus cardiomyocytes day 0 and §$P<0.05$ versus fibroblasts day 0 (**D**); ANOVA followed by Bonferroni multiple comparison test.

(Figure 1C). Cell cycle activity assessed by flow cytometry after 4′,6-diamidino-2-phenylindole (DAPI) labeling identified highest levels of DNA-synthesis in fibroblasts (17±1%) and cardiomyocytes (9±0.2%) on culture day 0 with lower but constant DNA synthesis levels during culture days 3–12 (fibroblasts: 7% to 10%; cardiomyocytes: 3% to 5%; n=4–8; Figure 1D). Interestingly, ^{3}H-thymidine incorporation dropped markedly ($P<0.05$) during the first 24 hours of EHT culture to increase first slowly (until culture day 5) and then markedly ($P<0.05$) on culture days 7–12 (Figure 1E). The steep increase in DNA synthesis in the absence of increasing cell numbers appeared to be the consequence of (1) cardiomyocyte binucleation (37±2%; n=4 EHTs, 30–40 cells each; Figure 1F) and (2) enhanced nuclear DNA content (polyploidy) in a subset of cardiomyocytes (>2N: 14±1%, n=4) in advanced EHT cultures (Online Figure II). These properties, together with a high RNA/DNA ratio and ^{3}H-phenylalanine incorporation (Online Figure III) appear to be signs of terminal differentiation and hypertrophic growth, suggesting advanced organotypic maturation in particular during late EHT culture.

Apoptotic Cell Death in Early EHT

The marked cell loss in EHT (Figure 1A) led us to investigate whether this was a consequence of apoptosis and represents a particular shortcoming of EHT versus conventional 2D cultures. Activated caspase-3, a surrogate for apoptosis, was especially high during early EHT culture (Figure 2A and Online Video IV). In agreement with this, high proapoptotic bax (Figure 2B) and low antiapoptotic Bcl-2 (Figure 2C) transcript abundances were observed, resulting in a markedly elevated bax/Bcl-2 ratio (Figure 2D). Notably, parallel cultures of EHT versus 2D showed similar levels of apoptosis (analyzed by flow cytometry), Trypan blue exclusion, and drop in cardiomyocyte number (Online Figure IV, A through C), collectively arguing against a unique apoptotic burden in EHT.

Lack of Evidence for Hypoxia in EHT

Hypoxia has been suggested as a limitation in tissue engineering and could have triggered apoptotic cell death. Surprisingly, we did not observe a regulation of highly sensitive hypoxia-response genes, for example, prolyl-4-hydroxylase domain isoforms 2 and 3 (prolyl-4-hydroxylase domain enzyme; PHD2/PHD3) mRNA and hypoxia-inducible factor-1α (HIF-1α) protein (Figure 3A through 3C). This led us to conclude that cells sensed normoxic conditions comparable to physiological tissue conditions throughout EHT culture and that elevated VEGF-A transcripts observed in late EHT culture (Figure 3D) were unrelated to hypoxia.

Sarcomere Maturation in EHT

A hallmark of maturation in terminally differentiated cardiomyocytes is the shift from a fetal to an adult gene expression program. This encompasses an increase in α-cardiac (α-cd) actin and a decrease in α-skeletal (α-sk) actin transcript concentration[10,18] as well as a shift from β-(fetal/slow)-MHC to α-(adult/fast)-MHC in rodents.[3,18] We could indeed observe an increase in α-cd actin and a parallel decrease in α-sk actin transcripts (Figure 4A and 4B), leading to an overall increase in total α-sarcomeric actin protein in late EHT-cultures (Figure 4C). In contrast, α-MHC transcript expression was unchanged, whereas β-MHC transcripts were elevated, resulting in a lower α-/β-MHC transcript ratio in EHT as compared with adult myocardium (7±2 versus 88±19-fold n=10/9; Figure 4D through 4F). Notably, also on protein level we identified a 4±0.8-fold (n=8) α-MHC excess in day 12 EHT (Figure 4F, inset). Direct comparison of atrial natriuretic peptide (ANP), α-sk actin, and α-cd actin transcript abundance in monolayer and EHT cultures documented that so called fetal genes (ANP, α-sk actin) were more abundant in monolayer as compared with EHT cultures (Online Figure V).

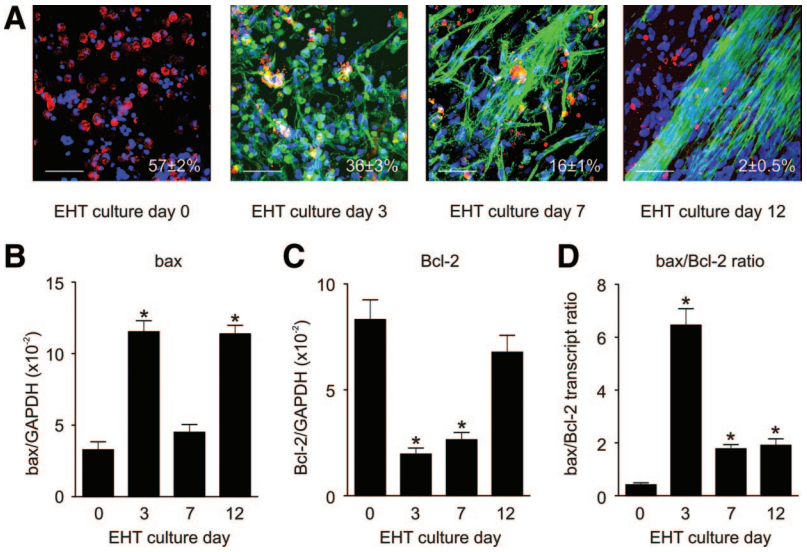

Figure 2. Apoptosis as main cause of cell death in EHT. **A**, Active caspase-3 (red) in EHTs; **bottom right**: percentage of caspase-positive cells at individual time points (green: f-actin; blue: DAPI-labeled nuclei; bars: 50 μm; refer also to Online Video IV). **B**, Bax (n=10/time point), and **C**, Bcl-2 (n=10/time point) transcripts per GAPDH transcript. **D**, Bax/Bcl-2 transcript ratio(n=10/time point). *$P<0.05$ versus day 0; ANOVA followed by Bonferroni multiple comparison test.

Dissection of the EHT Proteome

Increasing fluorescence intensity after α-actinin immunolabeling (in particular in day-12, EHT-derived cardiomyocytes; Online Figure I, A) provided additional evidence for tissue maturation. Subsequently, we performed proteome analyses to obtain a more comprehensive snapshot of the EHT proteome on culture days 0 and 12 (Figure 5A). The identity of a select set of proteins was confirmed by mass spectrometry (Online Table I). In agreement with the notion of advanced organotypic and in particular ventricular maturation in EHT, we observed a markedly enhanced level of the ventricular isoform of myosin light chain (MLC2v) protein per cardiomyocyte in day 12 versus day 0 EHTs (Figure 5B). Robust detection of tropomyosin isoforms, desmin, and M-type creatine kinase provided further evidence for the presence of cardiomyocytes with an advanced degree of maturation. Vimentin protein, characteristically expressed in fibroblasts, did not significantly change during EHT culture (Figure 5C), indicating phenotypic stability in this most abundant cellular constituent of EHT.

Structural Properties of EHT-Derived Cardiomyocytes

The shape and size of cardiomyocytes changed dramatically during EHT maturation from round and unstructured directly after isolation (mean diameter: 10±0.2 μm; volume: 570±32 μm^3, n=60) to rod-shaped and clearly cross-striated with sarcomeres in registry in 12-day-old EHTs (mean diameter: 5.8±0.1 μm, length: 72±2 μm, volume: 2,040±120 μm^3, n=113; Figure 6). Compared with cardiomyocytes from 12-day-old rats, EHT-derived cardiomyocytes acquired a similar length but were thinner and consequently less voluminous (mean diameter: 9.2±0.1 μm, length: 67±1 μm, volume: 4,724±154 μm^3, n=3 hearts, 80–100 cells each; Figure 6). Myocytes from adult rats were clearly larger than EHT- and 12-day-old, rat heart–derived myocytes (mean

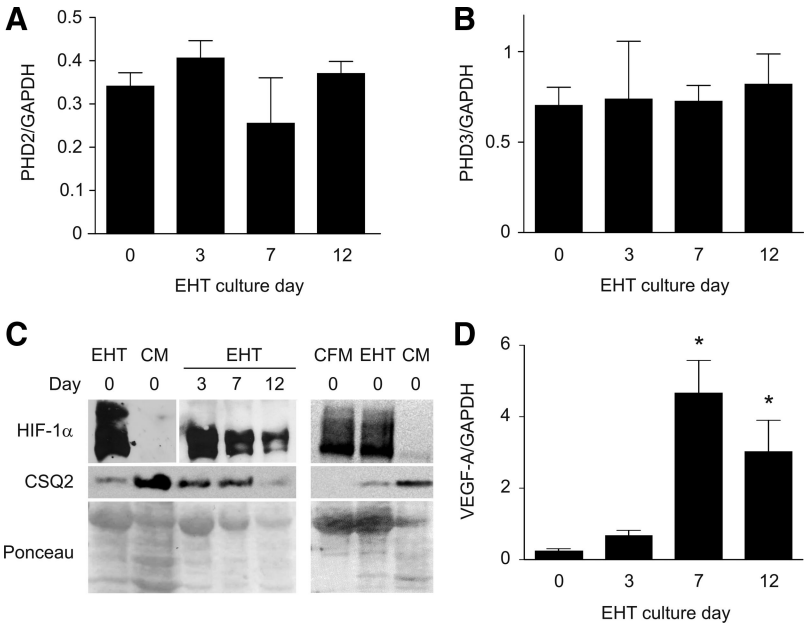

Figure 3. Lack of signs of intense hypoxia in EHT culture. **A**, PHD2, and **B**, PHD3 transcripts per GAPDH transcript during EHT culture (n=4/time point). **C**, HIF-1α protein in EHT at different time points in culture, in isolated cardiomyocytes (CM), and cell free EHT matrix (CFM, composed of collagen and Matrigel); note that CFM is high in HIF-1α protein (extracellular), which is gradually washed out during EHT culture; calsequestrin 2 (CSQ2) is displayed as cardiomyocyte housekeeping protein; equal amounts of protein were loaded. **D**, VEGF-A transcripts per GAPDH transcript (n=10) during EHT culture. *$P<0.05$ versus EHT day 0; ANOVA followed by Bonferroni multiple comparison test.

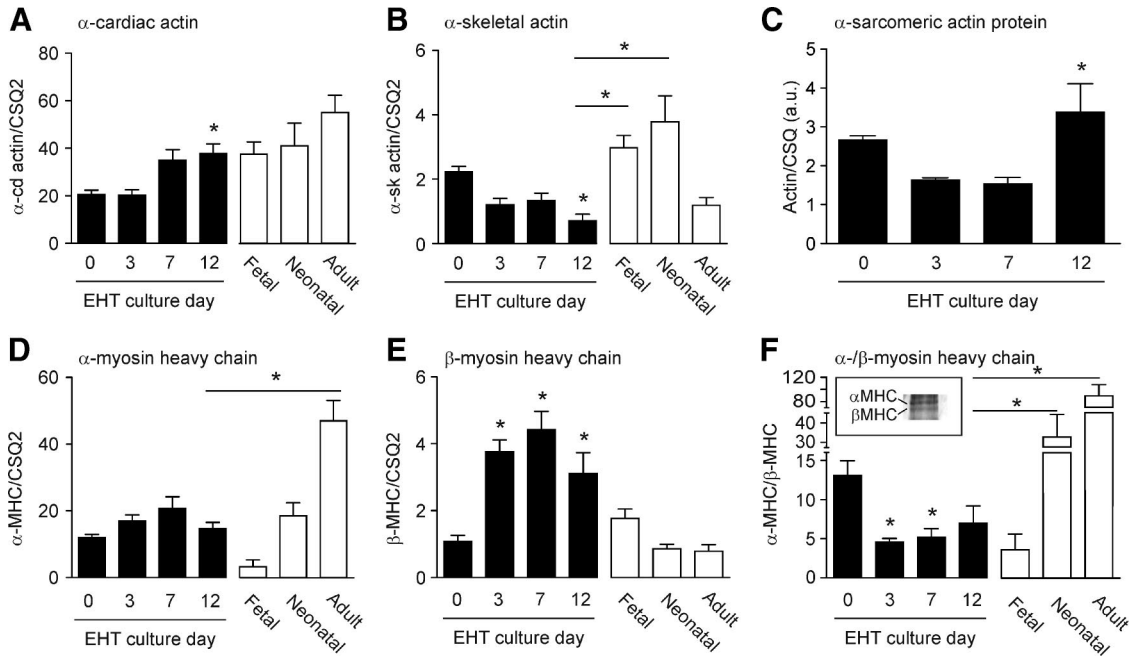

Figure 4. Molecular evidence for myocardial maturation in EHT. **A**, α-Cardiac (cd) actin (n=8–10/time point), and **B**, α-skeletal (sk) actin (n=7–10/time point) transcripts per calsequestrin 2 (CSQ2) transcript in EHT and rat myocardium. **C**, α-Sarcomeric actin protein content in EHT (indexed to CSQ2; n=9–12/time point). **D**, α-MHC (n=9–10/time point), and **E**, β-MHC (n=7–10/time point) transcripts per CSQ2 transcript in EHT and rat myocardium. **F**, α-/β-MHC transcript ratio in EHT and rat myocardium (n=10/time point). **Inset**: representative SYPRO Ruby–stained PAGE indicating α-/β-MHC protein composition in day 12 EHT. *$P<0.05$ versus EHT day 0 (**A, B, E,** and **F**) and EHT day 3 (**C**) or between indicated columns (in **B, D,** and **F**); ANOVA followed by Bonferroni multiple comparison test.

diameter: 24.7±0.4 μm, length: 114±1 μm, volume: 57 102± 1735 μm^3, n=3 hearts, 80–100 cells each; Figure 6). Mean diastolic sarcomere length was similar in all groups (EHT-derived: 1.85±0.04 μm [n=31]; day-12 rat heart: 1.83± 0.02 μm [n=28]; adult rat heart: 1.84±0.02 μm, [n=27]).

Organotypic Response of EHT to Hypertrophic Stimuli

We cultured EHTs during the maturation phase (culture days 7–12) in the presence of phenylephrine (20 μmol/L; PE) and angiotensin II (100 nmol/L; Ang) to assess their responsive-

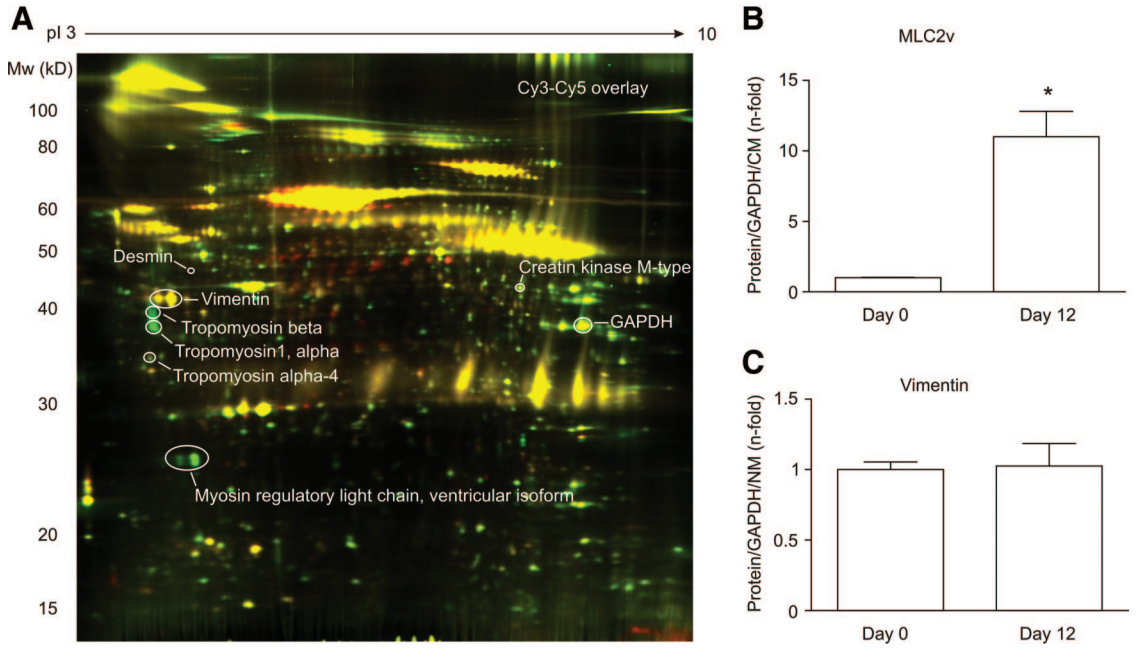

Figure 5. EHT proteome. **A**, Proteins were isolated from EHT (culture days 0 and 12) and separated by 2D electrophoresis using an immobilized pH gradient strip (3–10 nonlinear); overlay of day 0 EHT (Cy3-labeled; green) and day 12 EHT (Cy5-labeled; red); overlay: yellow. **B**, Abundance of ventricular MLC2 isoform (MLC2v) in day 0 and day 12 EHT (normalized to GAPDH and cardiomyocyte [CM] number; n=3/time-point). **C**, Abundance of vimentin in day 0 and day 12 EHT (normalized to GAPDH and nonmyocyte [NM] number; n=3/time point). *$P<0.05$; 2-tailed unpaired Student *t* test.

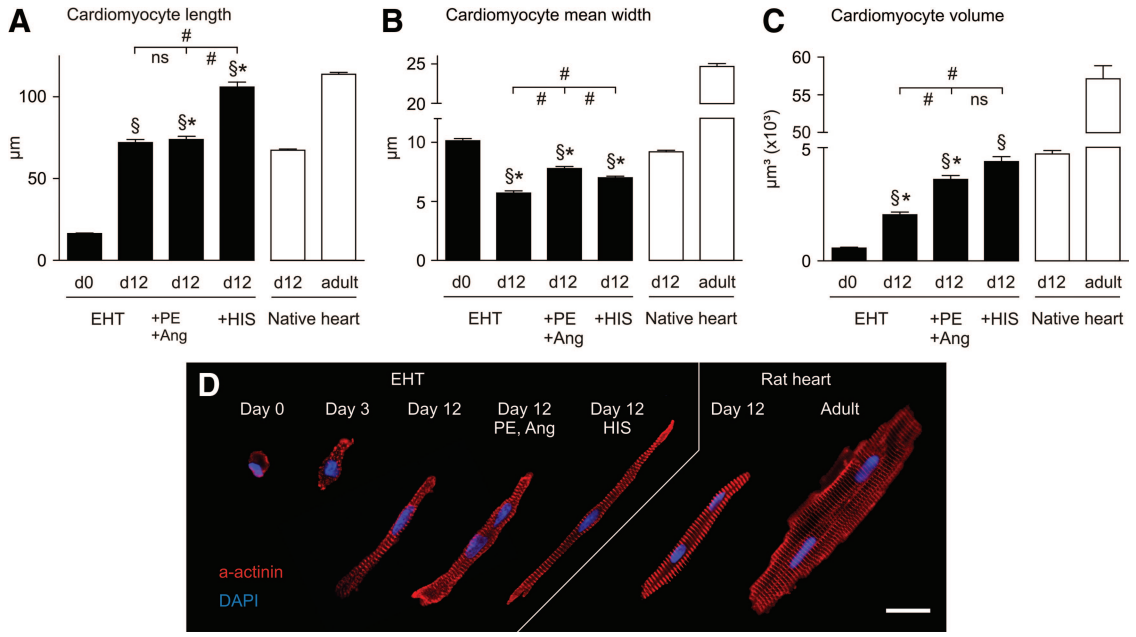

Figure 6. Hypertrophic cardiomyocyte growth in EHT and native heart. **A**, Length, **B**, mean width, and **C**, volume of EHT-derived cells at culture day 0 (n=60 cells) and day 12: (1) untreated (n=113 cells), (2) simulated neurohumoral overstimulation with phenylephrine (20 μmol/L; PE) and angiotensin-2 (100 nmol/L; Ang; n=111 cells), and (3) in the presence of hypertrophy-inducing serum (HIS; 10%; n=153 cells) during EHT culture days 7–12. Cell dimensions from postpartum day 12 (n=3 hearts, 80–100 cells each) and adult (n=3 hearts, 80–100 cells each) rat hearts are displayed for comparison. **D**, Immunostaining of cardiomyocytes from EHT culture days 0, 3, and 12 (untreated, PE/Ang, and HIS) and rat myocardium. Red: α-actinin, blue: DAPI-labeled nuclei; bar: 20 μm. The image is an assembly of individual photographs of representative cells from each group. *P<0.05 versus day-12 native heart; §P<0.05 versus EHT day 0; ANOVA followed by Bonferroni multiple comparison test.

ness to simulated neurohumoral overstimulation. Compared with standard medium conditions (EHT, day 12), we observed a concentric hypertrophy at the cellular level with a marked increase in cell width without major changes in cell length (Figure 6). During the course of these experiments, we also identified dramatic differences in responses to serum (10% in the culture medium) with "hypertrophy-inducing serum" (HIS), leading to a remarkable elongation of cardiomyocytes without major changes in cell width (Figure 6). These findings highlight the necessity for rigorous serum screens but also indicate the opportunity to use EHT for phenotypic screens to identify hypertrophy inducing secretomes and/or specific hypertrophic factors. Importantly, the phenotypic changes induced by PE/Ang and HIS were accompanied by distinct patterns of hypertrophic gene expression with particularly high ANP in HIS and low α/β-MHC ratio as well as high α-sk actin transcript abundance in PE/Ang treated EHTs (Figure 7).

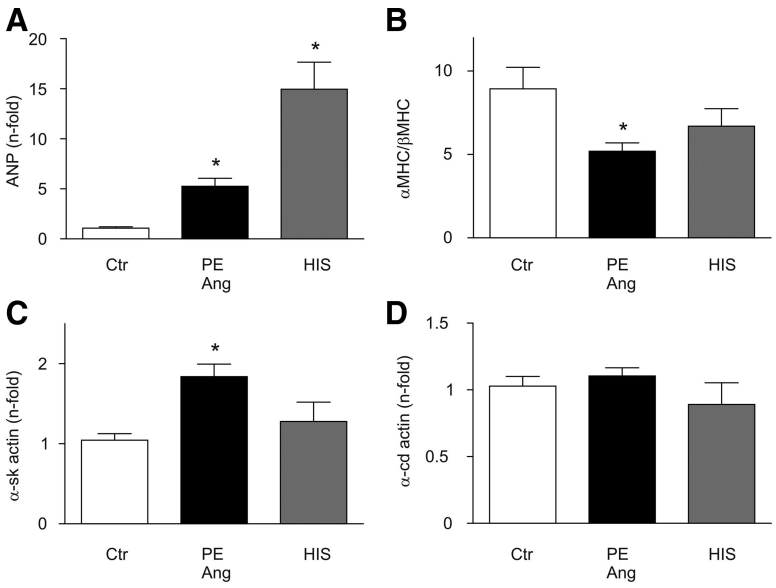

Figure 7. Fetal gene transcription program in "hypertrophic" EHT. **A**, ANP transcripts per calsequestrin 2 (CSQ2) transcript. **B**, α-/β-MHC transcript ratio. **C**, α-skeletal (sk) actin transcripts per CSQ2 transcript. **D**, α-cardiac (cd) actin transcripts per CSQ2 transcript. **White bars:** control EHTs; **black bars:** EHTs stimulated with 20 μmol/L phenylephrine and 100 nmol/L angiotensin-2 during culture days 7–12; **gray bars**: EHTs stimulated with HIS (10%) during culture days 7–12. Group size: n=7–10. *P<0.05 versus control (Ctr); ANOVA followed by Bonferroni multiple comparison test.

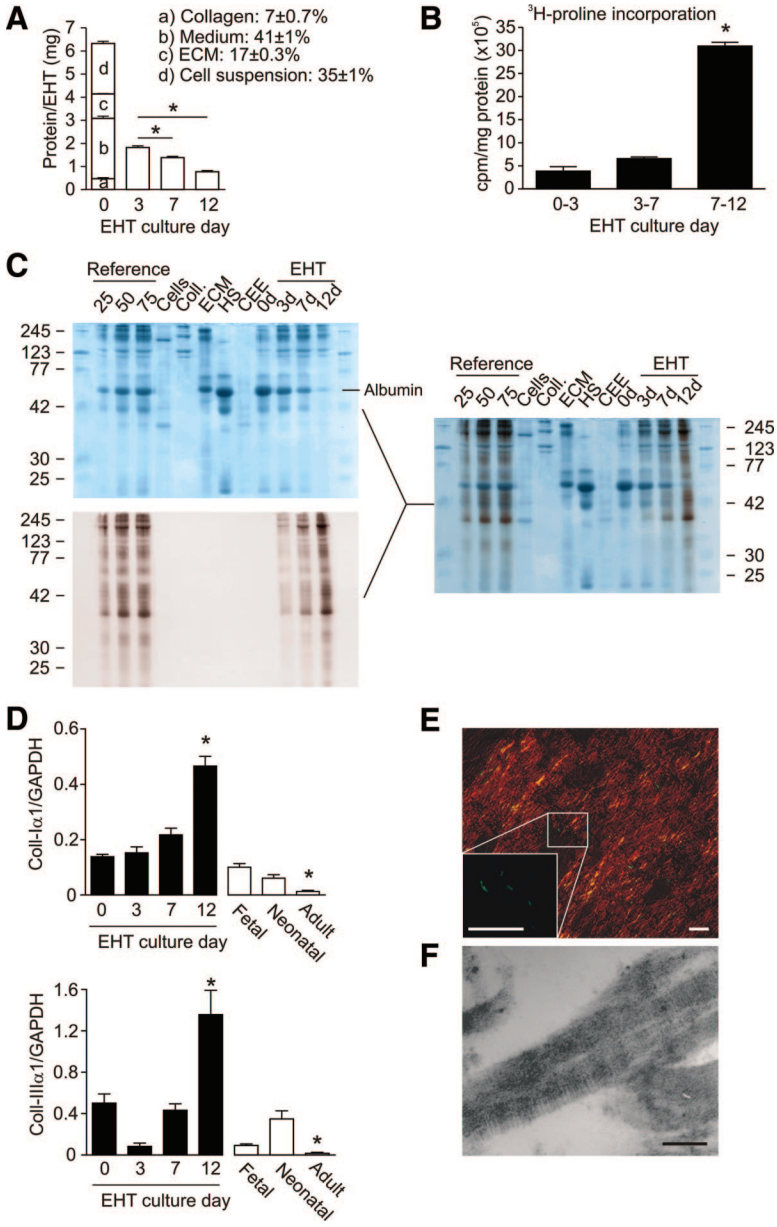

Figure 8. Intense ECM restructuring during EHT culture. **A**, Protein content of EHT at different time points during culture. The day 0 column indicates the contribution of collagen, culture medium ECM, and cell suspension (contains 23% cell protein and 77% serum protein) fractions to total EHT protein content at the time of casting. **B**, ^{3}H-proline incorporation in EHTs during culture days 0 to 3, 3–7, and 7–12 (n=7–8). **C**, PAGE separation of proteins from neonatal rat heart cells (Cells), collagen (Coll.), ECM, horse serum (HS), chick embryo extract (CEE), and EHT from culture days 0, 3, 7, and 12. EHTs were labeled with ^{35}S-cysteine/-methionine on culture days 3, 7, and 12 (**upper left panel:** Coomassie-stained PAGE; **lower left panel:** autoradiography; **right panel**: superimposition of Coomassie-stained PAGE and corresponding autoradiography; 25, 50, 75 μg of pooled day 3, 7, and 12 EHT-protein were loaded as reference). **D**, Collagen type I (Coll-I) and collagen type III (Coll-III) transcripts per GAPDH transcript in EHT and rat myocardium (n=8–10/time-point). **E**, Sirius red staining of collagen fibers: thick collagen fibers (orange); thin, newly synthesized collagen fibers (green; highlighted in **inset**; bars: 10 μm). **F**, Ultrastructure of collagen fiber in day 12 EHT with characteristic cross-striations; bar: 100 nm. *$P<0.05$ versus EHT day 3 (**A**), EHT days 0 to 3 (**B**), or EHT day 0 (**D**); ANOVA followed by Bonferroni multiple comparison test.

Intense Matrix Restructuring During EHT Culture

At the time of casting, EHT contained 0.5±0.05 mg rat tail collagen, 1.1±0.02 mg extracellular basement membrane protein, 2.7±0.1 mg serum protein (in 210 μL DMEM with 20% horse serum and 4% chick embryo extract), and a cell suspension containing 2.2±0.1 mg proteins (2.5×10^{6} cells in 377 μL DMEM with 10% fetal calf serum: cells, 0.5 mg; serum, 1.7 mg; n=4 in each group; Figure 8A). The nominal EHT protein content decreased from 6.4±0.1 mg (n=4) to 0.8±0.05 mg during culture (n=4; Figure 8A) despite elevated incorporation of ^{3}H-phenylalanine (Online Figure III, B), ^{3}H-proline (Figure 8B), and ^{35}S-methionine/cysteine (Figure 8C). Experiments with the latter isotope mixture demonstrated pronounced incorporation especially in 40-kDa and >200-kDa proteins probably resembling actin (molecular weight: 43 kDa; see also Figure 4C) and myosin/collagen (molecular weight: 220/290 kDa). High ^{3}H-proline incorporation (Figure 8B) and high collagen type I/III transcript levels (Figure 8D) at later stages of EHT culture provided further evidence for endogenous ECM synthesis during the EHT maturation phase (culture days 7–12). Sirius red staining documented thick collagen fibers (orange in polarized light) aligned along the major force axis in 12-day-old EHTs and thin collagen fibers (green in polarized light), which represent freshly synthesized collagen (Figure 8E). Additional evidence for de novo collagen matrix production stems from transmission electron microcopy, which identified cross-striated mature collagen (Figure 8F), being absent in the original collagen hydrogel. Cell loss (Figure 1A) and matrix disaggregation were apparently key factors for EHT protein loss, especially during EHT consolidation (culture days 0–7). Upregulation of matrix metalloproteinases (MMP-2 and MMP-14; Online Figure VI, A and B) and their tissue inhibitors (TIMP-1 and TIMP-2; Online Figure VI, C and D) supported the hypothesis of intense matrix restructuring. MMP-3 and MMP-13 could not be reliably detected in

neonatal rat heart cells (Ct values: >40 [MMP-3] and >35 [MMP-13]; n=10/target), but were clearly present at EHT-culture day 3 (Ct values: 28 [MMP-3] and 25 [MMP-13]; n=10/target), supporting the general concept of strong MMP-based matrix remodeling, especially at early time points of EHT culture.

Discussion

We investigated the hypothesis that immature rat cardiomyocytes undergo terminal differentiation and a process of advanced organotypic maturation in 3D EHT cultures and made the following key observations: (1) cardiomyocytes matured in EHT in a partially organotypic manner as indicated by the formation of a clearly anisotropic and cross striated rod-shaped cell morphology, abundant binucleation, and a fetal-to-adult actin isoform shift; (2) the ventricular MLC2 isoform was identified in EHT and strongly upregulated on protein level, providing further evidence for advanced ventricular maturation; (3) cardiomyocytes in EHTs responded to different hypertrophic stimuli with distinct morphological (concentric versus eccentric hypertrophy) and molecular (fetal gene expression) changes; (4) apoptosis in enzymatically isolated myocytes limited cell and especially cardiomyocyte survival in EHT; (5) EHT resembled normoxic tissue at all investigated time points; (6) matrix restructuring paralleled EHT-development and resulted in at least partial replacement of ECM constituents. Collectively, our data documents that the EHT culture format induces terminal differentiation and advanced maturation of initially immature cardiomyocytes to a "ventricle-like" phenotype in vitro. The process of EHT "development" can be classified as "EHT-consolidation" (culture days 0–7) followed by "EHT-maturation" (culture days 7–12). Demonstration of qualitatively different responses, for example, concentric versus eccentric hypertrophy, to distinct hypertrophic stimuli, for example, PE/Ang versus HIS, suggests that EHT can be exploited as a novel test-bed to dissect mechanisms of hypertrophic growth.

Using tissue-engineered myocardium as a model of myocardial development or in substance screening clearly depends on its close resemblance with bona fide heart muscle. Classical monolayer cultures display little structural, molecular, and also functional similarities with mature myocardium and do in general not respond reliably to hypertrophic stimuli, unless subject to inherently hostile serum starvation at low seeding density. Most notably, cardiomyocytes in monolayer cultures quickly lose their regular rod-shaped morphology and concomitantly reexpress fetal genes, indicating a molecular "resetting" to a prenatal state of development.[5–7] Growth on patterned substrates may partially improve this condition and support anisotropic growth[19,20]; yet, morphological and molecular data documenting advanced maturation and formation of 3D tissue on a macroscopic scale are limited.

Particular morphological hallmarks of advanced cardiomyocyte maturation are a rod-shaped geometry and binucleation. Cardiomyocytes enzymatically isolated from EHTs were rod-shaped and abundantly binucleated (37%), resembling to some degree a state of maturity observed in cardiomyocytes from 10- to 12-day-old rat hearts.[2,21,22] However, compared with heart-derived cardiomyocytes, EHT-derived cardiomyocytes were thinner (length/width ratio, 12:1 in EHT versus 7:1 in 12-day-old rat hearts and 5:1 in adult rat hearts). This difference in aspect ratio was at least in part "normalized" under PE and Ang stimulation (length/width ratio, 10:1; Figure 6) but also paralleled by a "mild" induction of ANP, all in the presence of "normal" serum. Interestingly, HIS caused marked cardiomyocyte elongation and ANP upregulation, responses which have been implicated in "pathological" hypertrophy. Although additional studies are warranted to establish phenotype "serome" relationships and identify distinct underlying mechanisms, we believe that our data provide compelling evidence for EHTs as a robust and nearly "physiological" in vitro system, which could be used, for example, to decipher the complex paracrine regulation of physiological versus pathological growth. In line with this notion, we could recently provide confirmatory evidence for the role of the MEK1-ERK1/2 pathway in concentric versus eccentric myocyte hypertrophy, conditions associated with pressure and volume overload, respectively, by making use of the EHT system.[23]

During physiological myocyte development, elongation of cardiomyocytes precedes parallel sarcomere assembly.[22,24] Subsequently, concentric hypertrophy, being the morphological correlate of parallel sarcomeric assembly, represents a compensatory mechanism to adapt to increasing load. Similarly, multinucleation and polyploidy have been reported to be enhanced under increasing load.[25] Accordingly, DNA synthesis (Figure 1D and 1E) was markedly elevated particularly after day 7 of EHT culture, that is, the time when EHTs were subjected to phasic stretch. Interestingly, enhanced DNA synthesis did not go along with an increase in myocyte or nonmyocyte cell number, suggesting load-induced karyokinesis, in the absence of palpable cytokinesis.

On the molecular level, the shift from skeletal to cardiac actin transcript expression (Figure 4A and 4B and Online Figure V) and the detection of elevated ventricular MLC2 in 12-day EHT (Figure 5B) provided further evidence for advanced organotypic maturation of cardiomyocytes in EHT. In apparent disagreement with this notion was the absence of the commonly reported massive β- to α-MHC transcript isoform shift. This may, however, be a consequence of the low (subphysiologic) endogenous beating frequency of EHT ($\approx$2 Hz), making faster actin-myosin kinetics dispensable. Whether electric stimulation of EHT at near physiological frequencies (6 Hz) would facilitate a shift from the observed $\approx$7-fold α-MHC transcript excess in spontaneously beating EHTs to a $\approx$88-fold excess as observed in adult heart muscle (Figure 4F), needs further investigation. Interestingly, PE/Ang and HIS lowered the α-/β-MHC transcript ratio, as anticipated under hypertrophy-inducing conditions.

Abundant caspase-3 activation and elevated bax expression suggested that apoptosis limited cell survival in EHT. It is important to note that caspase activation does not always lead to fully executed apoptosis with nuclear fragmentation but is also involved in reversible myofilament breakdown after cell isolation.[26] Induction of apoptosis during enzymatic cell isolation and cell loss during early culture are also commonly observed in monolayer cardiomyocyte cultures (Online Fig-

ure IV). This set of data collectively argues against the notion that the reported apoptosis represents a specific tissue engineering limitation. We could recently demonstrate that activation of prosurvival pathways such as the Akt pathway can protect cardiomyocytes in early EHT cultures from apoptosis.[27]

Hypoxia-induced apoptosis has been suggested as a main limitation for cell survival in tissue-engineered myocardium,[28] and we initially interpreted VEGF-A transcript elevation as a sign of chronic hypoxia in particular in later stages of EHT culture. However, more comprehensive investigations of more sensitive biomarkers for acute (HIF-1α) and chronic (PHD2/3) hypoxia did not provide any evidence in support of EHT hypoxia during culture. We emphasize that cardiomyocytes are physiologically exposed to oxygen pressure below 40 mm Hg, which corresponds to $<$5% ambient oxygen,[29] and that the provided oxygen supply (21% ambient oxygen) is apparently sufficient for normoxic EHT maintenance. Although the stimulus for enhanced VEGF-A expression has not been identified, one should consider that VEGF-A by itself may be cardioprotective[30] and in fact may be an important prerequisite for the observed rapid vascularization of EHT grafts in vivo.[31,32]

Of particular interest for in vivo applications in regenerative medicine is also the apparent replacement of the original hydrogel by endogenously produced ECM. This remodeling process is on the one hand crucial for the formation of mechanically stable EHTs. On the other hand, it provides a perspective for the generation of nonimmunogenic "therapeutic" EHTs from autologous cells.

Taken together, cardiomyocyte maturation in EHT compares favorably to myocyte maturation in monolayer culture and does to some extent simulate physiological development in vivo. The observed differences in cardiomyocyte size and MHC isoform composition may be a consequence of "subphysiologic" loading and low intrinsic contraction frequency and thus may be interpreted as a "physiological" response to partially unphysiologic culture conditions. Interestingly, concentric and eccentric hypertrophic growth could be stimulated in EHT using simulated neurohumoral/serum activation. These data in particular suggest that EHT may constitute a unique model system to study mechanisms governing hypertrophic growth in cardiomyocytes. As a consequence of the observed differentiation and maturation inducing capacity, EHT cultures may also find a novel application as in vitro test-bed to define the fate of progenitor cells in a tissue-like context.

Acknowledgments

We thank M. Bauer and N. Feifel for designing qPCR primer-probe sets, B. Endress for excellent technical assistance, and C. Perske for helping with light microscopy of Sirius red stained samples.

Sources of Funding

This study was supported by the German Research Foundation (DFG; Zi708/7–1, 8–1, 10–1, FOR604, and KFO155 to D.K., W.A.L., and W.H.Z.), the Federal Ministry for Education and Research (01GN 0520, 01GN0827, and 01GN0957 to W.H.Z.), the Deutsche Stiftung für Herzforschung (F29/03 to W.H.Z.), and the European Union (EU FP7 CARE-MI to W.H.Z.).

Disclosures

None.

References

1. Eschenhagen T, Zimmermann WH. Engineering myocardial tissue. *Circ Res*. 2005;97:1220–1231.
2. Katzberg AA, Farmer BB, Harris RA. The predominance of binucleation in isolated rat heart myocytes. *Am J Anat*. 1977;149:489–499.
3. Lompre AM, Nadal-Ginard B, Mahdavi V. Expression of the cardiac ventricular alpha- and beta-myosin heavy chain genes is developmentally and hormonally regulated. *J Biol Chem*. 1984;259:6437–6446.
4. Soonpaa MH, Kim KK, Pajak L, Franklin M, Field LJ. Cardiomyocyte DNA synthesis and binucleation during murine development. *Am J Physiol*. 1996;271:H2183–H2189.
5. Naito H, Melnychenko I, Didie M, Schneiderbanger K, Schubert P, Rosenkranz S, Eschenhagen T, Zimmermann WH. Optimizing engineered heart tissue for therapeutic applications as surrogate heart muscle. *Circulation*. 2006;114:I72–I78.
6. Weikert C, Eppenberger-Eberhardt M, Eppenberger HM. Cellular engineering of ventricular adult rat cardiomyocytes. *Cardiovasc Res*. 2003; 59:874–882.
7. Eppenberger-Eberhardt M, Flamme I, Kurer V, Eppenberger HM. Reexpression of alpha-smooth muscle actin isoform in cultured adult rat cardiomyocytes. *Dev Biol*. 1990;139:269–278.
8. Radisic M, Park H, Shing H, Consi T, Schoen FJ, Langer R, Freed LE, Vunjak-Novakovic G. Functional assembly of engineered myocardium by electrical stimulation of cardiac myocytes cultured on scaffolds. *Proc Natl Acad Sci U S A*. 2004;101:18129–18134.
9. Zimmermann WH, Schneiderbanger K, Schubert P, Didie M, Munzel F, Heubach JF, Kostin S, Neuhuber WL, Eschenhagen T. Tissue engineering of a differentiated cardiac muscle construct. *Circ Res*. 2002;90:223–230.
10. Carrier RL, Papadaki M, Rupnick M, Schoen FJ, Bursac N, Langer R, Freed LE, Vunjak-Novakovic G. Cardiac tissue engineering: cell seeding, cultivation parameters, and tissue construct characterization. *Biotechnol Bioeng*. 1999;64:580–589.
11. Leor J, Aboulafia-Etzion S, Dar A, Shapiro L, Barbash IM, Battler A, Granot Y, Cohen S. Bioengineered cardiac grafts: a new approach to repair the infarcted myocardium? *Circulation*. 2000;102:III56–III61.
12. Li RK, Jia ZQ, Weisel RD, Mickle DA, Choi A, Yau TM. Survival and function of bioengineered cardiac grafts. *Circulation*. 1999;100: II63–II69.
13. Bursac N, Loo Y, Leong K, Tung L. Novel anisotropic engineered cardiac tissues: studies of electrical propagation. *Biochem Biophys Res Commun*. 2007;361:847–853.
14. Engelmayr GC Jr, Cheng M, Bettinger CJ, Borenstein JT, Langer R, Freed LE. Accordion-like honeycombs for tissue engineering of cardiac anisotropy. *Nat Mater*. 2008;7:1003–1010.
15. Shimizu T, Yamato M, Isoi Y, Akutsu T, Setomaru T, Abe K, Kikuchi A, Umezu M, Okano T. Fabrication of pulsatile cardiac tissue grafts using a novel 3-dimensional cell sheet manipulation technique and temperature-responsive cell culture surfaces. *Circ Res*. 2002;90:e40.
16. Eschenhagen T, Fink C, Remmers U, Scholz H, Wattchow J, Weil J, Zimmermann W, Dohmen HH, Schafer H, Bishopric N, Wakatsuki T, Elson EL. Three-dimensional reconstitution of embryonic cardiomyocytes in a collagen matrix: a new heart muscle model system. *FASEB J*. 1997;11:683–694.
17. Zimmermann WH, Fink C, Kralisch D, Remmers U, Weil J, Eschenhagen T. Three-dimensional engineered heart tissue from neonatal rat cardiac myocytes. *Biotechnol Bioeng*. 2000;68:106–114.
18. Boheler KR, Carrier L, Chassagne C, de la Bastie D, Mercadier JJ, Schwartz K. Regulation of myosin heavy chain and actin isogenes expression during cardiac growth. *Mol Cell Biochem*. 1991;104:101–107.
19. McDevitt TC, Woodhouse KA, Hauschka SD, Murry CE, Stayton PS. Spatially organized layers of cardiomyocytes on biodegradable polyurethane films for myocardial repair. *J Biomed Mater Res A*. 2003;66: 586–595.
20. Feinberg AW, Feigel A, Shevkoplyas SS, Sheehy S, Whitesides GM, Parker KK. Muscular thin films for building actuators and powering devices. *Science*. 2007;317:1366–1370.
21. Li F, Wang X, Capasso JM, Gerdes AM. Rapid transition of cardiac myocytes from hyperplasia to hypertrophy during postnatal development. *J Mol Cell Cardiol*. 1996;28:1737–1746.
22. Anversa P, Olivetti G, Loud AV. Morphometric study of early postnatal development in the left and right ventricular myocardium of the rat, I:

hypertrophy, hyperplasia, and binucleation of myocytes. *Circ Res*. 1980; 46:495–502.
23. Kehat I, Davis J, Tiburcy M, Accornero F, Saba-El-Leil MK, Maillet M, York AJ, Lorenz JN, Zimmermann WH, Meloche S, Molkentin JD. Extracellular signal-regulated kinases 1 and 2 regulate the balance between eccentric and concentric cardiac growth. *Circ Res*. 2011;108: 176–183.
24. Olivetti G, Anversa P, Loud AV. Morphometric study of early postnatal development in the left and right ventricular myocardium of the rat, II: tissue composition, capillary growth, and sarcoplasmic alterations. *Circ Res*. 1980;46:503–512.
25. Engelmann GL, Vitullo JC, Gerrity RG. Age-related changes in ploidy levels and biochemical parameters in cardiac myocytes isolated from spontaneously hypertensive rats. *Circ Res*. 1986;58:137–147.
26. Communal C, Sumandea M, de Tombe P, Narula J, Solaro RJ, Hajjar RJ. Functional consequences of caspase activation in cardiac myocytes. *Proc Natl Acad Sci U S A*. 2002;99:6252–6256.
27. Vantler M, Karikkineth BC, Naito H, Tiburcy M, Didie M, Nose M, Rosenkranz S, Zimmermann WH. PDGF-BB protects cardiomyocytes from apoptosis and improves contractile function of engineered heart tissue. *J Mol Cell Cardiol*. 2010;48:1316–1323.
28. Radisic M, Malda J, Epping E, Geng W, Langer R, Vunjak-Novakovic G. Oxygen gradients correlate with cell density and cell viability in engineered cardiac tissue. *Biotechnol Bioeng*. 2006;93:332–343.
29. Whalen WJ. Intracellular pO2 in heart and skeletal muscle. *Physiologist*. 1971;14:69–82.
30. Das DK, Maulik N. Cardiac genomic response following preconditioning stimulus. *Cardiovasc Res*. 2006;70:254–263.
31. Zimmermann WH, Melnychenko I, Wasmeier G, Didie M, Naito H, Nixdorff U, Hess A, Budinsky L, Brune K, Michaelis B, Dhein S, Schwoerer A, Ehmke H, Eschenhagen T. Engineered heart tissue grafts improve systolic and diastolic function in infarcted rat hearts. *Nat Med*. 2006;12:452–458.
32. Zimmermann WH, Didie M, Wasmeier GH, Nixdorff U, Hess A, Melnychenko I, Boy O, Neuhuber WL, Weyand M, Eschenhagen T. Cardiac grafting of engineered heart tissue in syngenic rats. *Circulation*. 2002;106:I151–157.

Novelty and Significance

What Is Known?

- Tissue-engineered myocardium may be used as in vitro tool for drug development and as a surrogate for heart muscle for in vivo applications in myocardial repair.
- Cardiac myocytes dedifferentiate in culture, leading to a loss in organotypic cell morphology and reexpression of fetal genes.
- The validity of classical monolayer cultures as in vitro platform for modeling of hypertrophic cardiomyocyte growth is limited.

What New Information Does This Article Contribute?

- Engineered heart tissue (EHT) formation is a staged process comprising an early tissue consolidation phase with selection of the "fittest" myocytes and fibroblasts as well as comprehensive extracellular matrix (ECM) remodeling; this is followed by a phase of organotypic maturation.
- Organotypic maturation of cardiomyocytes in EHT includes terminal differentiation, abundant binucleation, development of an essentially rod-shaped morphology, and a fetal-to-adult shift in gene expression pattern.
- EHT may be useful in modeling of concentric versus eccentric cardiomyocyte hypertrophy.

Tissue engineering could potentially provide realistic heart muscle models and surrogate myocardium. However, cellular maturity in tissue-engineered myocardium has been sparsely documented. We show that a unique collagen hydrogel-based, cardiac tissue-engineering format, EHT, supports organotypic maturation in originally immature cardiomyocytes from neonatal rats. Our studies provide novel insight into the developmental properties of EHT, for example, hypertrophic growth under normoxic conditions and comprehensive ECM remodeling leading to replacement of the original hydrogel scaffold with ECM. The latter finding highlights the predicted but thus far undemonstrated capacity of the cardiac fibroblast to function as a key "engineer" in myocardial tissue engineering. We have established appropriate experimental conditions that differentially affect cardiomyocyte growth (ie, concentric hypertrophy under simulated neurohumoral activation and eccentric hypertrophy in the presence of hypertrophy-inducing serum). Collectively, the results of this study enhance the utility of the EHT technology as methodological bridge between classic 2D cell culture and animal models. It may represent a useful tool for identifying specific environmental cues that facilitate organotypic maturation of cardiomyocytes from human (stem) cell sources as well.

Supplement Material:

Terminal Differentiation, Advanced Organotypic Maturation, and Modeling of Hypertrophic Growth in Engineered Heart Tissue

*Malte Tiburcy[*1], Michael Didié[*1], Oliver Boy[1], Peter Christalla[1], Stephan Doeker[1], Hiroshi Naito[1], Bijoy Chandapillai Karikkineth[1], Ali El-Armouche[1], Michael Grimm[2], Monika Nose[2], Thomas Eschenhagen[2], Anke Zieseniss[3], Doerthe Katschinksi[3], Nazha Hamdani[4], Wolfgang A. Linke[4], Xiaoke Yin[5], Manuel Mayr[5] & Wolfram-Hubertus Zimmermann[1]*

[1]Department of Pharmacology, Georg-August-University Goettingen, Germany; [2] Institute of Experimental and Clinical Pharmacology, University Medical Center Hamburg-Eppendorf, Germany; [3]Department of Cardiovascular Physiology, Georg-August-University Goettingen, Germany; [4]Department of Cardiovascular Physiology, Institute of Physiology, Ruhr University Bochum, Germany; [5]King's BHF Centre, King's College, University of London, United Kingdom

EXPANDED MATERIALS AND METHODS

Experimental animals were maintained in accordance with the guiding principles of the American Physiological Society. Animal experiments were approved by the local authorities (Regierung von Mittelfranken: 621.2531.31-2/00 and -17/01; BWG of the Freie und Hansestadt Hamburg; Niedersächsisches Landesamt für Verbraucherschutz und Lebensmittelsicherheit).

EHT construction and treatment. Heart cells were isolated from neonatal rats (postnatal days 1-3) using a fractionated DNase/Trypsin digestion protocol without preplating to maintain the original cardiomyocyte:non-myocyte composition[1, 2]. EHTs (reconstitution volume: 0.9 ml) were prepared by pipetting a mixture containing the isolated heart cells ($2.5x10^6$ cells in DMEM with 10% fetal calf serum, 1 mmol/l glutamine, 100 U/ml penicillin, and 100 µg/ml streptomycin), pH-neutralized collagen type I from rat tails (0.5 mg/EHT – measured by the Sircol Collagen Assay; Biocolor), basement membrane protein containing Engelbreth-Holm-Swarm tumor exudate (10% v/v; BD Biosciences), and concentrated serum-containing culture medium (2xDMEM, 20% horse serum, 4% chick embryo extract, 200 U/ml penicillin, and 200 µg/ml streptomycin) in circular molds (inner diameter, 8 mm; outer diameter, 16 mm; height, 5 mm^3). Spontaneously beating EHTs were transferred to stretch devices on culture day 7 to continue culture under phasic load (from 100 to 110% of slack length at 2 Hz) for additional 5 days. EHTs were treated with 20 µmol/L phenylephrine and 100 nmol/L angiotensin-II from day 7-12 with daily medium change to induce hypertrophy. For 2D culture experiments neonatal heart cells were seeded in 6-well plates ($5x10^5$/well) coated with the EHT matrix (diluted 1:50 in PBS) and cultured in parallel to EHTs in standard primary cardiomyocyte culture medium (DMEM, 10% fetal calf serum, 100 µmol/L 5-bromo-2'-deoxyuridine, 100 U/ml penicillin, and 100 µg/ml streptomycin).

^{3}H-thymidine incorporation. EHTs were maintained in standard culture medium with 1 µCi/ml ^{3}H-thymidine for 6 hours on the indicated culture days. After washing in ice cold PBS, EHTs were dissolved in ice cold lysis buffer (10 mmol/L trishydroxylaminomethane [Tris; pH 8], 1 mmol/L ethylene-diamine-tetraacetic acid [EDTA; pH 8], 0.1% sodium dodecyl sulfate [SDS]) followed by 6 h proteinase K (0.1 µg/µl) digestion at 55 °C. DNA was precipitated in isopropanol after DNase-free RNase treatment (0.02 µg/µl for 60 min at 37 °C) and protein extraction in potassium acetate solution (3 mol/L potassium/5 mol/L acetate). After washing in 70% ethanol, DNA was resuspended in Tris/EDTA-buffer (100 mmol/L Tris, 10 mmol/L EDTA; pH 7.6). DNA content was measured by spectrophotometry and ^{3}H-activity was assessed by liquid scintillation counting.

Cell isolation from EHT. EHTs were immersed in modified Bicarbonate-Free Hanks' Balanced Salt Solution with HEPES (BFHH; NaCl 136.9 mmol/L, KCl 5.36 mmol/L, $MgSO_4$ 0.81 mmol/L, glucose 5.55 mmol/L, $CaCl_2$ 0.0125 mmol/L, KH_2PO_4 0.44 mmol/L, Na_2HPO_4 0.34 mmol/L, HEPES 20 mmol/L) containing 0.035 mg/ml Liberase Blendzyme III (Roche) and 30 mmol/L BDM (2,3-

butanedione monoxime) at 37 °C for 60 min. Enzymatic activity was stopped by addition of 10% FBS, 5 mmol/L EDTA. Isolated cells were fixed for immunostaining or flow cytometry as described below.

Histology. EHTs or dispersed single cells were fixed in neutral buffered 4% formaldehyde/1% methanol, pH 7.4 with 30 mmol/L BDM and subjected either to light (LM) or confocal laser scanning (CLSM; Zeiss 510 Meta or 710/NLO LSM) microscopy, as described recently [3]. Cryo-sections (10 µm; Leica CM3050 S) were stained with phalloidin-Alexa 488 (3.3 U/ml; Molecular Probes) to label f-actin, DAPI (4',6-diamidino-2-phenylindole; 1 µg/ml) to label nuclei, and antibodies directed against α-actinin (1:1000; Sigma), and activated caspase-3 (1:250; Promega) with appropriate secondary antibodies. For Sirius red staining EHTs were embedded in paraffin, and sectioned at a thickness of 6 µm. After de-waxing in Roti-Histol (Roth) for 2x 15 min, the sections were hydrated through a decreasing ethanol series and washed with distilled water for 2x 5 min. Sections were incubated for 60 min in a solution of 0.5 g Sirius red F3B (C.I. 35782) in 500 ml of saturated aqueous solution of picric acid, briefly washed in acidified water (5 ml glacial acetic acid per liter of distilled water), dehydrated and mounted in Histokitt. Sections were then subjected to polarized light microscopy (Olympus BX41). Green and red channels were separated by setting a threshold in the green-red distribution using the CIE lab function of ImageJ. Respective images of above and below threshold signals as well as merged image were computed applying identical settings. For transmission electron microscopy (TEM) EHTs were fixed in 2.5% glutaraldehyde (in PBS with 1 mmol/L $CaCl_2$ and 30 mmol/L BDM) overnight at 4°C. After extensive washing in PBS, EHTs were postfixed for 2 h in osmiumtetroxyd/PBS (1:1). After epon embedding, ultrathin sections (50 nm) were cut (Ultracut UCT, Leica), contrasted with uranyl acetate and lead citrate, and imaged with a Zeiss Leo 906 EM.

Flow cytometry. Dispersed cells from neonatal rat (P0-3) and EHTs at different time-points were fixed in ice-cold 70% ethanol. Staining for α-actinin (Sigma) or vimentin (Abcam) was performed in the presence of 0.5% Triton-X at 4°C for 45 min. Appropriate secondary antibodies were applied for 30 min at room temperature. Negative controls were incubated with the secondary antibody alone. DNA was stained with DAPI (1 µg/ml). Samples were run on a LSRII cytometer and analysed with FacsDiva software (BD Biosciences). The gating strategy to exclude cell clumps and multinucleated cells was based on the width of the DAPI signal. DNA content/cell cycle was analyzed using ModFit LT 3.2 software (Verity).

Cell isolation from native heart. After an intra-peritoneal bolus injection of heparin (500 IU) 12 day and 12 week old Wistar rats were euthanized. Hearts were quickly excised and cells were isolated using a modified Langendorff method[4]. Briefly, hearts were digested with 0.1 mg/ml Liberase Blendzyme III (Roche) in oxygenized perfusion buffer (NaCl 113 mmol/L, KCl 4.7 mmol/L, KH_2PO_4 0.6 mmol/L, Na_2HPO_4 0.6 mmol/L, $MgSO_4$ 1.2 mmol/L, $NaHCO_3$ 12 mmol/L, $KHCO_3$ 10 mmol/L, HEPES 10 mmol/L, taurine 30 mmol/L, glucose 5.55 mmol/L, BDM 10 mmol/L, calcium 0.0125 mmol/L). Single cells were fixed for immunostaining as described above.

RNA/DNA isolation and quantitative RT-PCR (qPCR). RNA and DNA were isolated using the Trizol®-method (Invitrogen) and quantified by spectrophotometry. cDNA was prepared from 2 µg total RNA by reverse transcription with MMLV-RT (Invitrogen) utilizing random hexamere primers (Roche) following standard protocols (Invitrogen). qPCR was performed in a 384 well format ABI prism HT 7900 system (Applied Biosystems) using gene-specific primers and fluorogenic probes (5' FAM and 3' TAMRA; **Online Table II**) as described earlier[5], unless indicated otherwise (see below). The reaction mixture contained 20 ng input cDNA, 3 mmol/l $MgCl_2$, 0.4 µmol/l forward and reverse primer, 0.5 µmol/l probe, 0.8 mmol/l NTP (Applied Biosystems), and 0.05 U TaqGold polymerase (Applied Biosystems) in a total volume of 10 µl supplemented with TaqPolymerase buffer II (Applied Biosystems). We used following temperature protocol: 30 sec at 50 °C and 10 min at 95 °C followed by 45 cycles of 30 sec at 95 °C and 1 min at 58 °C. GAPDH expression was similar in all study groups and was therefore employed to normalize for differences in RNA quantity and RT-efficiency. Cardiomyocyte-specific transcript quantity was indexed to the expression of muscle specific calsequestrin 2 (CSQ2). The linearity of each PCR was confirmed by analyzing serial cDNA

dilutions, prepared from total RNA isolated from neonatal rat hearts. Quantification of transcripts was performed using the Standard Curve algorithm[6]. PHD2 and PHD3 mRNA levels were quantified using 1 µl of cDNA (Fermentas) and a SYBR Green qPCR reaction kit (Clontech) in combination with a MX3000P light cycler (Stratagene) as described before[7]. The initial template concentration of each sample was calculated by comparison with serial dilutions of a calibrated standard. Primer sequences: PHD2 forward TACAGGATAAACGGCCGACAC and PHD2 reverse GGCTTGAGTTCAACCCTCAC; PHD3 forward GTTAACCCGAGACTGGACGA and PHD3 reverse CATACCGCTAGGCTTTGCTC.

Development of a cardiomyocyte specific qPCR assay. To better account for cardiomyocyte loss we developed a PCR-assay allowing the quantification of 17,500-1,750,000 cardiomyocytes in a mixed heart cell population, based on the detection of muscle specific calsequestrin 2 (CSQ2) transcripts (**Online Figure VII**). We designed intron-spanning fluorogenic TaqMan probes (5' FAM, 3' TAMRA) and adjacent primer pairs to amplify muscle specific CSQ2, GAPDH, and 18S-RNA. Rat heart cells were isolated as described and cardiomyocytes were enriched by preplating, resulting in a cell suspension containing 70% cardiomyocytes as identified by α–sarcomeric actinin labeling[2]. Subsequently, heart cells were mixed with defined numbers of cardiac non-myocytes. Non-myocytes were prepared by propagating a quickly adhering cell fraction from the original neonatal rat heart cell isolate. This cell fraction was grown to subconfluency (70%), trypsinized, frozen in 7.5% DMSO-containing cell culture medium, thawed, and re-grown. This procedure was repeated at least twice, yielding heart cell cultures free of beating or non-beating cardiomyocytes. Cell mixtures were subjected to RNA isolation (Trizol®, Invitrogen). Reverse transcription and qPCR were performed as described with different quantities of input cDNA (20 pg and 20 ng) to demonstrate that cardiomyocytes express constant levels of CSQ2 transcripts. This was further confirmed with two different CSQ2 primer-probe sets (see below). Similar cDNA loading was confirmed by GAPDH and 18S-RNA transcript analyses:

CSQ2: NCBI accession#: AF001334
Forward: TTT CTG ACG GAG ACG TTC AGG
Probe: TGG CTG CCT ACA GTA CGC TGG GAA C
Reverse: TAG CAG GAC AGA GAG GGT GCA

CSQ2: Ensemble accession#: ENSRNOG00000016243
Forward: CCA AGA GGC TGG GCT TCA G
Probe: CGA TCT CTA CTG GGT CCT CAA TGA GGT CCA A
Reverse: CCT CAT TCT TGA AAA AGC CAA GC

GAPDH: NCBI accession#: NC005103
Forward: AAC TCC CTC AAG ATT GTC AGC AA
Probe: ATG GAC TGT GGT CAT GAG CCC TTC CA
Reverse: CAG TCT TCT GAG TGG CAG TGA TG

18S-RNA: NCBI accession#: V01270
Forward: ACG ACC CAT TCG AAC GTC
Probe: CCT ATC AAC TTT CGA TGG TAG TCG CCG T
Reverse: CTT GGA TGT GGT AGC CGT TT

Immunoblotting. EHTs were washed thoroughly in ice cold PBS and rapidly homogenized in lysis buffer containing 30 mmol/L Tris (pH 8.8), 5 mmol/L EDTA (pH 8), 3% SDS, 10% glycerol, 30 mmol/L NaF, and 2 µg/ml aprotinin or 4 mmol/L urea, 140 mmol/L Tris (pH 6.8), 1% SDS, 2% Nonidet P-40, and protease inhibitors (Roche Applied Science). After centrifugation at 13,000 g for 10 min, supernatants containing soluble proteins were subjected to protein concentration measurement using modified Lowry or Bradford methods, respectively. Equal amounts of protein (30-100 µg) were resolved by SDS-PAGE and transferred onto polyvinylidene fluoride (sarcomeric actin) or nitrocellulose (HIF-1α, calsequestrin) membranes by semidry blotting. Primary antibodies used were:

anti-sarcomeric actin (clone 5C5; Sigma), anti-HIF-1α (Novus, NB100-479), anti-calsequestrin 2 (AffinitiBioReagents). Primary antibodies were detected with appropriate horseradish peroxidase coupled secondary antibodies. Sarcomeric actin immunocomplexes were enhanced with the ECL-plus kit (Amersham Biosciences) and recorded with a ChemiDoc system (Syngene). Signals were quantified with Gene-Tools software (Syngene). For detection of HIF-1α membranes were incubated with 100 mmol/L Tris-HCl (pH 8.5), 2.65 mmol/L H_2O_2, 0.45 mmol/L luminol, and 0.625 mmol/L coumaric acid for 1 min. Chemiluminescence signals were detected with the LAS-3000 Image Reader (Fujifilm).

Detection of myosin heavy chain isoforms. To assess myosin heavy chain isoform composition EHTs were homogenized in sample buffer containing 50 mmol/L Tris-HCl (pH 6.8), 5 mmol/L EDTA, 10% glycerol, 8 µg/ml leupeptin, 1% beta-mercaptoethanol, 20% SDS, 0.1% (w/v) dithiothreitol, 6 µmol/L bromophenol blue, and washing buffer (5 mmol/L Tris-EDTA, pH 8.0). The separating gel contained 7.5% total acrylamide (acrylamide to bis-acrylamide ratio, 30:0.8), the stacking gel contained 4% total acrylamide. To check for linearity, different amounts of EHT (0.5–3.0 µg) were loaded and the densities of the myosin heavy chain bands were analyzed; a load of 1.5 µg per lane was selected as it was found to be within the linear range. After separation of proteins, gels were stained overnight with SYPRO Ruby (Molecular Probes). Fixation and washing were performed according to the manufacturer's guidelines. Gels were digitized using LAS-4000 Image Reader (Fujifilm; 460 nm/605 nm E_x/E_m) and signals were analyzed using Multi Gauge software (Fujifilm).

2D electrophoresis (2-DE). EHT samples were homogenized in 9 mol/L urea, 1% DTT, 4% CHAPS, protease and phosphatase inhibitors (Complete Mini, Roche), and 0.8% Pharmalytes 3-10. For difference in-gel electrophoresis (DIGE), proteins were precipitated (ReadyPrep 2D Clean-up kit, Biorad) and re-suspended using a lysis buffer (30 mmol/L TrisCl pH 8.5, 8 mol/L urea, 4% w/v CHAPS) compatible with DIGE labelling (GE healthcare). After centrifugation at 13,000 g for 10 min, the supernatant containing soluble proteins was harvested and the protein concentration was determined using a modification of the method described by Bradford. The fluorescence dye labelling reaction was carried out at a dye/protein ratio of 200 pmol/L / 50 µg. After incubation on ice for 30 min, the labelling reaction was stopped by scavenging non-bound dyes with 10 mmol/L lysine (L8662, Sigma) for 15 min. Protein extracts (50 µg/sample) were loaded on nonlinear immobilized pH gradient (IPG) 18-cm strips, pH 3-10 (GE Healthcare) using an in-gel rehydration method. Loaded IPG-strips were rehydrated in 8 mol/L urea, 0.5% w/v CHAPS, 0.2% w/v DTT, and 0.2 % w/v Pharmalyte pH 3-10 overnight in a reswelling tray. Strips were isoelectrically focused at 0.05 mA/IPG-strip and 35 kVh at 20 °C (IPGphor, GE healthcare) and subsequently equilibrated in 6 mol/L urea containing 30% v/v glycerol, 2% w/v SDS, and 0.01% w/v bromphenol blue, with addition of 1% w/v DTT for 15 min, followed by the same buffer without DTT, but with the addition of 4.8% w/v iodoacetamide for 15 min. Large-format gradient gels (5-10% stack, 10-16% linear, 16-20% stack) were cast using a 2-DE optimizer (NextGen Sciences, Huntingdon, UK). Gels were subsequently overlaid with water-saturated butanol (2:3) and left to polymerize overnight. SDS-PAGE was performed using the Ettan DaltSix system (GE healthcare). After electrophoresis, fluorescence images were acquired by using the Ettan DIGE Imager (GE Healthcare) with the following parameters: exposure time: Cy2, 0.8 sec, Cy3, 0.3 sec, Cy5, 0.5 sec, pixel size: 0.1 mm. Images were analyzed by DeCyder software (version 7.0, GE Healthcare). The 2-DE gels were fixed overnight in methanol:acetic acid:water solution (4:1:5 v/v/v) and visualized by silver staining using the Plus one silver staining kit (GE healthcare) without glutaraldehyde to ensure compatibility with subsequent mass spectrometry analysis. Silver-stained gels were scanned in transmission scan mode using a calibrated scanner (GS-800, Biorad).

Nanoflow liquid chromatography tandem mass spectrometry (LC-MS/MS). Gel pieces containing selected protein spots were treated overnight with modified trypsin (Promega) according to a published protocol modified for use with an Investigator ProGest (Genomic Solutions) robotic digestion system[8]. Following enzymatic degradation, peptides were separated by a nanoflow HPLC system on a reverse-phase column (Acclaim PepMap100, C18, 25cm, 5µm, 100Å, Dionex) and applied to a LTQ ion-trap mass spectrometer (Thermo Fisher Scientific) with electron transfer

dissociation (ETD). Spectra were collected from the ion-trap mass analyzer using full ion scan mode over the mass-to-charge (m/z) range 450-2000. MS-MS scans were performed on each ion using dynamic exclusion and alternating collision-induced dissociation (CID) and ETD. Database search was performed using the SEQUEST (Thermo Fisher Scientific) and X! Tandem software. Two missed cleavages per peptide were allowed and carbamidomethylation of cysteine as well as partial oxidation of methionine were assumed. Peptide identifications were accepted if they could be established at greater than 95% probability as specified by the Peptide Prophet algorithm. Protein identifications were accepted if they could be established at greater than 99% probability with at least two independent peptides.

^{3}H-phenylalanine and ^{3}H-proline incorporation. EHTs were maintained in standard culture medium with 1 µCi/ml ^{3}H-phenylalanine or ^{3}H-proline as indicated. Protein was precipitated in 10% ice-cold trichloroacetic acid (TCA) at 4 °C over night. The supernatant was collected and subjected to liquid scintillation counting to assess the non-incorporated fraction of the isotopes. The protein precipitate was washed twice in ice-cold PBS, suspended in 1 mmol/L NaOH containing 0.01% SDS for 2 h at 37 °C, and subjected to liquid scintillation counting. Total protein content was analyzed by a modified Lowry-Assay (Bio-Rad DC Protein Assay).

^{35}S-cysteine/-methionine incorporation, PAGE, and autoradiography. EHTs were cultured in cysteine- and methionine-free EHT culture medium with 4.5 g/l glucose for 6 h and subsequently incubated for 18 h in fresh cysteine- and methionine-free EHT culture medium supplemented with 100 µCi/ml ^{35}S-cysteine/-methionine on the indicated culture days. EHT protein was prepared and quantified as described above. Similar quantities of total proteins were loaded on 7% SDS-polyacrylamide gels and separated electrophoretically. Gels were stained with Coomassie blue, immersed in Amplify Fluorographic solution (Amersham Biosciences), vacuum dried, and subjected to autoradiography on intensifier screens (Expo Hyperfilm; Amersham Biosciences) for 6.5 h at -80 °C.

Statistical analyses. Data are presented as mean ± standard error of the mean (SEM). Statistical differences were determined using two-sided, unpaired Student's *t*-tests or one-way analysis of variance (ANOVA) followed by Bonferroni's multiple comparison test. A P value < 0.05 was considered statistically significant.

Supplementary References

1. Zimmermann WH, Fink C, Kralisch D, Remmers U, Weil J, Eschenhagen T. Three-dimensional engineered heart tissue from neonatal rat cardiac myocytes. *Biotechnol Bioeng.* 2000;68:106-114
2. Naito H, Melnychenko I, Didie M, Schneiderbanger K, Schubert P, Rosenkranz S, Eschenhagen T, Zimmermann WH. Optimizing engineered heart tissue for therapeutic applications as surrogate heart muscle. *Circulation.* 2006;114:I72-78
3. Zimmermann WH, Schneiderbanger K, Schubert P, Didie M, Munzel F, Heubach JF, Kostin S, Neuhuber WL, Eschenhagen T. Tissue engineering of a differentiated cardiac muscle construct. *Circ Res*. 2002;90:223-230
4. Pohlmann L, Kroger I, Vignier N, Schlossarek S, Kramer E, Coirault C, Sultan KR, El-Armouche A, Winegrad S, Eschenhagen T, Carrier L. Cardiac myosin-binding protein c is required for complete relaxation in intact myocytes. *Circ Res*. 2007;101:928-938
5. Weil J, Zolk O, Griepentrog J, Wenzel U, Zimmermann WH, Eschenhagen T. Alterations of the preproenkephalin system in cardiac hypertrophy and its role in atrioventricular conduction. *Cardiovasc Res*. 2006;69:412-422
6. Livak KJ, Schmittgen TD. Analysis of relative gene expression data using real-time quantitative pcr and the 2(-delta delta c(t)) method. *Methods*. 2001;25:402-408
7. Holscher M, Silter M, Krull S, von Ahlen M, Hesse A, Schwartz P, Wielockx B, Breier G, Katschinski DM, Zieseniss A. Cardiomyocyte-specific prolyl-4-hydroxylase domain 2 knock out protects from acute myocardial ischemic injury. *J Biol Chem*. 2011;286:11185-11194

8. Shevchenko A, Jensen ON, Podtelejnikov AV, Sagliocco F, Wilm M, Vorm O, Mortensen P, Boucherie H, Mann M. Linking genome and proteome by mass spectrometry: Large-scale identification of yeast proteins from two dimensional gels. *Proc Natl Acad Sci U S A.* 1996;93:14440-14445

ONLINE FIGURE/TABLE/VIDEO LEGENDS

Online Table I. Protein identifications by tandem mass spectrometry (LC-MS/MS). The amino acid sequences and scores of the identified peptides are provided. The blue color highlights the number of unique peptides, unique spectra, total spectra, and the sequence coverage as obtained by CID. The corresponding values for ETD (if applicable) are given below, but are not highlighted.

Online Table II. qPCR primers and probes.

Online Figure I. Quantification of cardiomyocytes and fibroblasts during EHT culture by flow cytometry. Representative plots identify distinct α-actinin- (**A**) and vimentin-positive cell populations (**B**) at the indicated days of EHT culture. Panels resemble overlays of individual dot plots: in red cell pools labeled for actinin (**A**) or vimentin (**B**); in grey cell pools exposed to secondary antibody only.

Online Figure II. DNA content in mononucleated cardiomyocytes and non-myocytes during EHT culture assessed by flow cytometry. A, Representative plots of DNA content in mononucleated cardiomyocytes (actinin-positive, red) and non-myocytes (actinin-negative, dark grey) at day 0 and day 12 of EHT culture. **B**, Fractions of mononucleated cardiomyocyte (top panel) and non-myocyte (lower panel) populations at day 0 (n=6) and day 12 (n=4) of EHT culture with 2N, 4N, and 8N DNA content.

Online Figure III. **Surrogate parameters suggesting hypertrophic growth in EHTs. A**, RNA/DNA ratio in EHTs on culture days 0 (n=18), 3 (n=19), 7 (n=10), and 12 (n=16). **B**, ^{3}H-phenylalanine incorporation during EHT culture days 0-3 (n=7), 3-7 (n=8), and 7-12 (n=5). **P*< 0.05 vs. EHT day 0 (**A**) and EHT days 0-3 (**B**); ANOVA and Bonferroni's multiple comparison test.

Online Figure IV. **Cell death in EHT and monolayer (2D) culture. A**, Analysis of DNA content in EHT- and 2D culture-derived cells (n=3 each). Sub-G1 fraction (green) denotes dead/apoptotic cells with condensed nuclei. **B**, Trypan-blue exclusion in EHT- and 2D culture-derived cells at culture day 1 (n=5 [EHT], n=4 [2D]). **C**, Comparison of CSQ2 transcript abundance in EHT (black bars) vs. 2D culture (white bars), n=5-6/time-point. **P*<0.05 vs. day 0 (grey bar); ANOVA and Bonferroni's multiple comparison test.

Online Figure V. Molecular markers of maturation in monolayer (2D) vs. EHT culture. A, ANP transcripts per GAPDH transcript; **B**, skeletal actin transcripts per GAPDH transcript; **C**, cardiac actin transcripts per GAPDH transcript in isolated neonatal heart cells at day 0 (black bars; n=5), 2D cultured cells at day 12 (blue bars; n=6), and EHT at day 12 (green bars; n=5). **D**, Correlation of cardiac and skeletal actin transcript abundance in freshly isolated neonatal heart cells (d0; black), in 2D culture (culture days 3,7, and 12 [left panel]) and EHT culture (culture days 3, 7, and 12 [middle panel]) - black arrows denote the trend in expression pattern change in 2D and EHT culture; right panel: direct comparison of 12 day 2D vs. EHT cultures and neonatal cardiomyocytes. *P<0.05 2D vs. EHT; Student's t-test.

Online Figue VI. ECM restructuring during EHT development. A, matrix metalloprotease-2 (MMP-2; n=8-10); **B**, MMP-14 (n=7-10); tissue inhibitor of matrix metalloprotease-1 (**C**, TIMP-1; n=7-10), and TIMP-2 (**D**; n=7-10) transcripts per GAPDH transcript in EHT and native rat heart tissue. **P*<0.05 vs. EHT day 0; ANOVA followed by Bonferroni's multiple comparison test.

Online Figure VII. Development of a cardiomyocyte-specific qPCR assay to allow approximation of cardiomyocyte content in mixed cell populations. Detection of CSQ2 (NCBI accession#: AF001334; squares) and GAPDH (NCBI accession#: NC005103; circles) transcripts in $2.5x10^6$ cells containing the indicated cardiomyocyte fraction by qPCR. High Ct-values indicate low transcript abundance. Symbols indicate individual Ct-values. Bars indicate the respective means. A Ct-value difference of 3.3 ideally represents a 10-fold difference in transcript abundance. Similar data could be obtained using alternative primer-probe pairs for muscle specific CSQ2 (Ensemble accession#: ENSRNOG00000016243) or 18S-RNA (NCBI accession#: V01270).

Online Video I: Spontaneous contractions in EHTs on culture day 3.
Online Video II: Spontaneous contractions of EHTs on culture day 7.
Online Video III: Spontaneous contractions of EHTs on culture day 12.
Online Video IV: Animated 3D reconstruction of adjacent optical sections from EHTs on culture days 0, 3, 7, and 12.

Online Table I

Database Set: 2 Databases

Database Name: a subset of the uniprot_sprot database
Taxonomy: All Entries
Number of Proteins: 193
Database Name: the uniprot_sprot.fasta.hdr database
Taxonomy: All Entries
Number of Proteins: 267354

Search Engine Set: 2 Search Engines

Search Engine: Sequest
Version: 27, rev. 12
Samples: All Samples
Fragment Tolerance: 1.00 Da (Monoisotopic)
Parent Tolerance: 2.0 Da (Monoisotopic)
Fixed Modifications: +57 on C (Carbamidomethyl)
Variable Modifications: +16 on M (Oxidation)
Database: the uniprot_sprot.fasta.hdr database (267354 entries)
Digestion Enzyme: Trypsin
Max Missed Cleavages: 2
Search Engine: X! Tandem
Fragment Tolerance: 1.00 Da (Monoisotopic)
Parent Tolerance: 2.0 Da (Monoisotopic)
Fixed Modifications: +57 on C (Carbamidomethyl)
Variable Modifications: +16 on M (Oxidation)
Database: a subset of the uniprot_sprot database
Digestion Enzyme: Trypsin
Max Missed Cleavages: 2

Scaffold Version: Scaffold-01_06_19

Peptide Thresholds: 95.0% minimum
Protein Thresholds: 99.0% minimum and 2 peptides minimum

Protein name	Protein accession numbers	Protein molecular weight	Protein identificatio	Number of un	Number of un	Number of tot	Percentage of	Percentage se	Peptide sequence	Previous amin	Next amino ac	Best Peptide i	Best SEQUES'	Best SEQUES'	Best X! Tande	Number of ide	Number of ide	Number of ide	Number of ide	Number of en	Calculated Pep	Peptide start i	Peptide stop index
Nidogen-1 precursor (Entactin) - Mus musculus (Mouse)	NID1_MOUSE	136603,6	100,00%	4	5	5	0,21%	4,10%	ASLHGGEPTTIIR	R	Q	95,00%	2,61	0,356	-0,146	0	1	1	0	2	1351,7336	1003	1015
									QTITFQECAHDDAR	R	P	95,00%	3,01	0,233	0	0	1	0	0	2	1691,745	609	622
									TNSVIAMDLAISK	K	E	95,00%	2,82	0,274	-0,699	0	1	0	0	2	1378,7252	1168	1180
									VLFDTGLVNPR	R	G	95,00%	2,73	0,0978	1,96	0	1	0	0	2	1230,6848	1055	1065
			99,80%	2	2	2	0,08%	2,17%	ASLHGGEPTTIIR	R	Q	95,00%	4,08	0,322	0	0	0	1	0	2	1351,7336	1003	1015
									QTITFQECAHDDAR	R	P	95,00%	2,97	0,152	0	0	1	0	0	2	1691,745	609	622
Collagen alpha-1(I) chain precursor (Alpha-1 type I collagen) - Mus musculus (Mouse	CO1A1_MOUSE	138014,7	100,00%	2	2	2	0,09%	2,00%	DRDLEVDTTLK	R	S	95,00%	2,56	0,38	-1,04	0	1	0	0	2	1304,6702	1215	1225
									GETGPAGPAGPIGPAGAR	R	G	95,00%	2,96	0,446	0,553	0	1	0	0	2	1532,7826	1056	1073
Vinculin (Metavinculin) - Mus musculus (Mouse)	VINC_MOUSE	116701,4	100,00%	9	9	9	0,36%	10,60%	AGEVINQPMMMAAR	K	Q	95,00%	2,9	0,184	0,0506	0	1	0	0	2	1566,7079	890	903
									ALASQLQDSLK	R	D	95,00%	3,06	0,377	2,33	0	1	0	0	2	1173,6481	571	581
									DPNASPGDAGEQAIR	R	Q	95,00%	2,9	0,297	-0,301	0	1	0	0	2	1497,6936	286	300
									LLAVAATAPPDAPNR	K	E	95,00%	2,11	0,27	-0,699	0	1	0	0	2	1476,8176	608	622
									MLGQMTDQVADLR	K	A	95,00%	3,1	0,391	0	0	1	0	0	2	1509,7043	327	339
									MSAEINEIIR	K	V	95,00%	2,05	0,146	1,72	0	1	0	0	2	1191,6044	237	246
									MTGLVDEAIDTK	K	S	95,00%	2,85	0,268	0	0	1	0	0	2	1308,636	709	720
									QVATALQNLQTK	K	T	95,00%	2,69	0,348	0,337	0	1	0	0	2	1314,7383	465	476
									VMLVNSMNTVK	R	E	95,00%	2,77	0,231	1,89	0	1	0	0	2	1267,6388	189	199
			100,00%	3	3	3	0,12%	3,57%	ALASQLQDSLK	R	D	95,00%	3,02	0,24	0	0	1	0	0	2	1173,6481	571	581
									LLAVAATAPPDAPNR	K	E	95,00%	2,7	0,279	0	0	1	0	0	2	1476,8176	608	622
									QVATALQNLQTK	K	T	95,00%	3,22	0,196	0	0	1	0	0	2	1314,7383	465	476
Nidogen-1 precursor (Entactin) - Mus musculus (Mouse)	NID1_MOUSE	136603,6	100,00%	12	17	18	0,78%	11,80%	AECLNPAQPGR	R	R	95,00%	2,75	0,217	2,75	0	1	0	0	2	1212,5797	1131	1141
									ASLHGGEPTTIIR	R	Q	95,00%	3	0,431	1,85	0	2	0	0	2	1351,7336	1003	1015
									CECVEGYHFSDR	R	G	95,00%	3,16	0,343	0,0269	0	1	0	0	2	1558,6055	734	745
									CGNHAVCNNLPGTFR	R	C	95,00%	2,27	0,172	-0,146	0	1	0	0	2	1716,77	719	733
									GDGQTCYDIDECSEQPSR	R	C	95,00%	3,65	0,422	0	0	1	0	0	2	2116,8188	701	718
									PGYQGDGFR	K	C	95,00%	2,49	0,343	0	0	1	0	0	2	996,454	828	836
									QAEVTFLGHPGK	R	L	95,00%	2,66	0,463	3,09	0	1	0	0	2	1283,675	517	528
									QCVAEGSPQR	R	V	95,00%	0	0	3,6	0	1	0	0	2	1114,4954	422	431
									QTITFQECAHDDAR	R	P	95,00%	3,32	0,406	0	0	1	0	0	2	1691,745	609	622
									TIFWTDSQLDR	R	I	95,00%	3,59	0,433	0,921	0	2	0	0	2	1381,6753	1032	1042
									VLFDTGLVNPR	R	G	95,00%	2,96	0,274	2,57	0	4	0	0	2	1230,6848	1055	1065
									YALSNSIGPVR	R	D	95,00%	2,41	0,357	2,29	0	2	0	0	2	1176,6377	649	659
			100,00%	5	6	6	0,26%	4,98%	ASLHGGEPTTIIR	R	Q	95,00%	3,16	0,273	0	0	2	0	0	2	1351,7336	1003	1015
									CGNHAVCNNLPGTFR	R	C	95,00%	3,47	0,289	0	0	0	1	0	2	1716,77	719	733
									PGYQGDGFR	K	C	95,00%	2,52	0,229	0	0	1	0	0	2	996,454	828	836
									QTITFQECAHDDAR	R	P	95,00%	3,77	0,253	0	0	1	0	0	2	1691,745	609	622
									YALSNSIGPVR	R	D	95,00%	2,84	0,291	0	0	1	0	0	2	1176,6377	649	659
Nidogen-1 precursor (Entactin) - Mus musculus (Mouse)	NID1_MOUSE	136603,6	100,00%	14	14	15	0,61%	13,50%	AECLNPAQPGR	R	R	95,00%	2,13	0,037	1,38	0	1	0	0	2	1212,5797	1131	1141
									ASLHGGEPTTIIR	R	Q	95,00%	2,52	0,104	6,37	0	0	1	0	2	1351,7336	1003	1015
									CECVEGYHFSDR	R	G	95,00%	3,2	0,327	0,181	0	1	0	0	2	1558,6055	734	745
									CGNHAVCNNLPGTFR	R	C	95,00%	3,17	0,335	0,181	0	1	0	0	2	1716,77	719	733
									EHILGAAGGADAQR	R	P	95,00%	3,23	0,37	0	0	1	0	0	2	1365,6876	852	865
									GNLYWTDWNR	R	D	95,00%	2,33	0,147	-0,544	0	1	0	0	2	1324,6074	1074	1083
									NGFSITGGEFTR	K	Q	95,00%	2,34	0,313	0,0555	0	1	0	0	2	1285,6178	505	516
									NLYYTDWK	K	T	95,00%	1,68	0,146	1,03	0	1	0	0	2	1102,521	1160	1167
									PGPGTQFTCECSIGFR	R	G	95,00%	2,49	0,319	0	0	1	0	0	2	1813,8004	685	700
									QAEVTFLGHPGK	R	L	95,00%	3,35	0,42	2,43	0	1	0	0	2	1283,675	517	528
									TIFWTDSQLDR	R	I	95,00%	3,13	0,421	1,14	0	1	0	0	2	1381,6753	1032	1042
									VIIGLAFDCVDK	K	V	95,00%	2,63	0,418	0,495	0	1	0	0	2	1349,7142	977	988
									VLFDTGLVNPR	R	G	95,00%	2,62	0,168	3,35	0	1	0	0	2	1230,6848	1055	1065
									YALSNSIGPVR	R	D	95,00%	2,47	0,244	1,51	0	2	0	0	2	1176,6377	649	659
								5,22%	ASLHGGEPTTIIR	R	Q	95,00%	3,75	0,305	0	0	0	1	0	2	1351,7336	1003	1015
									CGNHAVCNNLPGTFR	R	C	95,00%	2,53	0,262	0	0	1	0	0	2	1716,77	719	733
									EHILGAAGGADAQR	R	P	95,00%	2,99	0,324	0	0	1	0	0	2	1365,6876	852	865
									QAEVTFLGHPGK	R	L	95,00%	2,94	0,264	0	0	1	0	0	2	1283,675	517	528
									YALSNSIGPVR	R	D	95,00%	2,59	0,251	0	0	1	0	0	2	1176,6377	649	659
Nidogen-1 precursor (Entactin) - Mus musculus (Mouse)	NID1_MOUSE	136603,6	100,00%	4	5	5	0,23%	3,94%	AECLNPAQPGR	R	R	95,00%	2,55	0,283	3,26	0	1	0	0	2	1212,5797	1131	1141
									CPDNTLGVDCIER	R	-	95,00%	2,79	0,302	0	0	1	0	0	2	1548,679	1232	1244
									EHILGAAGGADAQR	R	P	95,00%	1,83	0,326	0	0	1	0	0	2	1365,6876	852	865
									YALSNSIGPVR	R	D	95,00%	2,76	0,325	3,05	0	2	0	0	2	1176,6377	649	659
Nidogen-1 precursor (Entactin) - Mus musculus (Mouse)	NID1_MOUSE	136603,6	100,00%	7	11	11	0,48%	6,67%	AECLNPAQPGR	R	R	95,00%	2,24	0,217	1,75	0	1	0	0	2	1212,5797	1131	1141
									ASLHGGEPTTIIR	R	Q	95,00%	2,71	0,401	1,39	0	1	2	0	2	1351,7336	1003	1015
									CECVEGYHFSDR	R	G	95,00%	2,79	0,286	-0,806	0	1	0	0	2	1558,6055	734	745
									CPDNTLGVDCIER	R	-	95,00%	2,56	0,278	-0,82	0	1	0	0	2	1548,679	1232	1244
									NGFSITGGEFTR	K	Q	95,00%	2,49	0,313	0,0915	0	1	0	0	2	1285,6178	505	516
									VLFDTGLVNPR	R	G	95,00%	2,8	0,376	2,28	0	1	0	0	2	1230,6848	1055	1065
									YALSNSIGPVR	R	D	95,00%	0	0	3,8	0	3	0	0	2	1176,6377	649	659

Serotransferrin precursor (Transferrin) (Siderophilin) (Beta-1 metal-binding globulin)	TRFE_HORSE	78076,6	100,00%	21	34	35	1,30%	31,30%	AACVCQELHNQQASYGK	K	N	95,00%	4,79	0,471	2,21	0	2	0	0	2	1963,8756	621	637
									AVSNFFAGSCVPCADR	K	T	95,00%	3,47	0,422	0,602	0	1	0	0	2	1757,774	165	180
									CGLVPVLAENYETR	K	S	95,00%	3,32	0,407	0,0269	0	1	0	0	2	1620,8058	423	436
									CLADGAGDVAFVK	K	H	95,00%	3,35	0,248	1,55	0	2	0	0	2	1322,6417	215	227
									DCYLASIPSHAVVAR	K	S	95,00%	3,56	0,433	0,721	0	2	0	0	2	1658,8324	261	275
									DDTQCLANLQPTTTYK	R	T	95,00%	3,29	0,0889	3,29	0	0	1	0	2	1868,8705	660	675
									DEYQLLCR	R	D	95,00%	2,09	0,163	2,55	0	2	0	0	2	1096,51	242	249
									DFHLFSSPHGK	K	D	95,00%	1,65	0,181	2,33	0	2	0	0	2	1271,6173	302	312
									EDIRPEVPKDECK	R	K	95,00%	3,01	0,355	0,509	0	2	0	0	2	1614,78	349	361
									FCLFQSATK	K	D	95,00%	2,53	0,199	3,37	0	2	0	0	2	1101,5404	646	654
									GDVAFVK	A	H	95,00%	1,83	0,124	1,52	1	0	0	0	2	735,4042	221	227
									KNSNFQLNQLQGK	K	K	95,00%	3,91	0,191	0,796	0	1	1	0	2	1518,803	119	131
									LLEACTFHRV	R	-	95,00%	2,51	0,322	2,59	0	1	0	0	2	1245,6415	697	706
									NSNFQLNQLQGK	K	K	95,00%	3,39	0,283	0	0	1	0	0	2	1390,708	120	131
									SIVPAPPLVACVKR	K	T	95,00%	0	0	2,82	0	0	1	0	2	1506,8832	45	58
									SKDFHLFSSPHGK	K	D	95,00%	3,24	0,351	0,131	0	1	0	0	2	1486,7445	300	312
									SSSDPDLTWNSLK	K	G	95,00%	3,02	0,433	4,55	0	1	0	0	2	1449,6863	457	469
									TSYLECIK	R	A	95,00%	2,12	0,176	1,85	1	1	0	0	2	1013,4979	59	66
									WCTVSNHEVSK	R	C	95,00%	2,75	0,173	0,796	0	1	0	0	2	1346,6162	25	35
									YLTAVANLR	K	Q	95,00%	1,32	0,261	1,39	1	4	0	0	2	1020,5842	682	690
									YYGYTGAFR	R	C	95,00%	2,2	0,178	2,14	0	2	0	0	2	1097,5056	541	549
		100,00%	10	12	12	0,45%	19,10%	AACVCQELHNQQASYGK	K	N	95,00%	4,2	0,348	0	0	2	0	0	2	1963,8756	621	637
									CACSNHEPYFGYSGAFK	K	C	95,00%	2,62	0,294	0	0	1	0	0	2	1994,8165	198	214
									CLADGAGDVAFVK	K	H	95,00%	3,38	0,297	0	0	1	0	0	2	1322,6417	215	227
									DCYLASIPSHAVVAR	K	S	95,00%	3,1	0,295	0	0	1	0	0	2	1658,8324	261	275
									DDTQCLANLQPTTTYK	R	T	95,00%	4,49	0,348	0	0	0	1	0	2	1868,8705	660	675
									HQTVEQNTDGRNPDDWAK	K	D	95,00%	4,32	0,304	0	0	0	1	0	2	2110,9544	562	579
									KNSNFQLNQLQGK	K	K	95,00%	4,54	0,162	0	0	1	1	0	2	1518,803	119	131
									NSNFQLNQLQGK	K	K	95,00%	3,99	0,285	0	0	1	0	0	2	1390,708	120	131
									SKDFHLFSSPHGK	K	D	95,00%	3,26	0,227	0	0	1	0	0	2	1486,7445	300	312
									SSSDPDLTWNSLK	K	G	95,00%	2,82	0,304	0	0	1	0	0	2	1449,6863	457	469
Aconitate hydratase, mitochondrial precursor (EC 4.2.1.3) (Citrate hydro-lyase) (Aco	ACON_RAT	85418,1	100,00%	9	12	12	0,48%	14,90%	ADIANLAEEFK	R	D	95,00%	1,94	0,14	2,01	0	1	0	0	2	1220,6165	313	323
									IVYGHLDDPANQEIER	K	G	95,00%	2,55	0,301	-0,342	0	1	0	0	2	1868,9144	69	84
									LEAPDADELPR	K	S	95,00%	2,33	0,159	0,62	0	1	0	0	2	1225,6067	524	534
									LTGTLSGWTSPK	K	D	95,00%	3,02	0,348	1	0	1	0	0	2	1247,6638	234	245
									NAVTQEFGPVPDTAR	R	Y	95,00%	2,59	0,342	-0,146	0	2	0	0	2	1601,7926	634	648
									NINIVR	K	K	95,00%	1,71	0,0453	1,43	1	0	0	0	2	728,4418	51	56
									SQFTITPGSEQIR	K	A	95,00%	3	0,391	0,62	0	1	0	0	2	1463,7495	412	424
									VGLIGSCTNSSYEDMGR	R	S	95,00%	2,64	0,428	0	0	2	0	0	2	1845,8113	379	395
									WVVIGDENYGEGSSR	R	E	95,00%	3,25	0,366	0,367	0	2	0	0	2	1667,7666	657	671
		100,00%	4	4	4	0,16%	7,56%	LTGTLSGWTSPK	K	D	95,00%	3,32	0,259	0	0	1	0	0	2	1247,6638	234	245
									SDFDPGQQTYQHPPK	R	D	95,00%	3,26	0,386	0	0	0	1	0	2	1731,7618	535	549
									VGLIGSCTNSSYEDMGR	R	S	95,00%	2,3	0,363	0	0	1	0	0	2	1845,8113	379	395
									WVVIGDENYGEGSSR	R	E	95,00%	2,39	0,213	0	0	1	0	0	2	1667,7666	657	671
Moesin (Membrane-organizing extension spike protein) - Homo sapiens (Human)	MOES_HUMAN	67803,8	100,00%	3	4	4	0,20%	4,85%	ALELEQER	R	K	95,00%	1,53	0,0845	2,54	0	2	0	0	2	987,5112	372	379
									AQMVQEDLEK	K	T	95,00%	2,85	0,123	1,54	0	1	0	0	2	1206,5677	449	458
									AQQELEEQTR	K	R	95,00%	2,86	0,258	1,1	0	1	0	0	2	1231,592	361	370
Pyruvate kinase isozymes M1/M2 (EC 2.7.1.40) (Pyruvate kinase muscle isozyme) - I	KPYM_RAT	57800,6	100,00%	6	8	9	0,38%	11,90%	AATESFASDPILYR	R	P	95,00%	2,62	0,393	0	0	1	0	0	2	1540,7648	93	106
									APIIAVTR	R	N	95,00%	1,67	0,279	1,92	1	0	0	0	2	840,5308	448	455
									GDYPLEAVR	K	M	95,00%	2,61	0,339	2,54	0	1	0	0	2	1019,5163	368	376
									GIFPVLCK	R	D	95,00%	1,87	0	2,96	0	1	0	0	2	933,5234	468	475
									LDIDSAPITAR	R	N	95,00%	2,95	0,403	4,85	0	2	0	0	2	1171,6326	33	43
									NTGIICTIGPASR	R	S	95,00%	2,23	0,256	0	0	3	0	0	2	1359,7057	44	56
Pyruvate kinase isozymes M1/M2 (EC 2.7.1.40) (Pyruvate kinase muscle isozyme) - I	KPYM_RAT	57800,6	100,00%	5	8	9	0,41%	9,61%	APIIAVTR	R	N	95,00%	1,65	0,178	1,43	1	0	0	0	2	840,5308	448	455
									EAEAAVFHR	R	L	95,00%	2,09	0,106	3,37	0	1	0	0	2	1029,5118	384	392
									ITLDNAYMEK	K	C	95,00%	1,82	0,348	2,01	0	3	0	0	2	1213,5776	142	151
									LDIDSAPITAR	R	N	95,00%	2,97	0,154	1,5	0	1	0	0	2	1171,6326	33	43
									NTGIICTIGPASR	R	S	95,00%	3,73	0,384	2,09	0	3	0	0	2	1359,7057	44	56
T-complex protein 1 subunit gamma (TCP-1-gamma) (CCT-gamma) - Bos taurus (Bo	TCPG_BOVIN	60569,2	100,00%	2	2	2	0,09%	4,22%	AVAQALEVIPR	R	T	95,00%	2,94	0,208	2,39	0	1	0	0	2	1166,6898	439	449
									TLIQNCGASTIR	R	L	95,00%	3,53	0,371	-0,447	0	1	0	0	2	1333,6899	450	461
Fascin (Singed-like protein) - Mus musculus (Mouse)	FSCN1_MOUSE	54490,2	100,00%	4	4	4	0,19%	9,13%	FLVVAHDDGR	R	W	95,00%	2,13	0,11	1,21	0	1	0	0	2	1128,5802	91	100
									LSCFAQSVSPAEK	R	W	95,00%	3	0,152	1,37	0	1	0	0	2	1423,6892	119	131
									YFGGTEDR	R	L	95,00%	0	0	2,75	0	1	0	0	2	944,4114	111	118
									YLAADKDGNVTCER	R	E	95,00%	2,66	0,326	0	0	1	0	0	2	1611,7439	69	82
Septin-11 - Homo sapiens (Human)	SEP11_HUMAN	49381,1	100,00%	3	3	3	0,16%	10,00%	AAAQLLQSQAQQSGAQQTK	K	K	95,00%	3,56	0,451	0	0	1	0	0	2	1957,0105	400	418
									FESDPATHNEPGVR	K	L	95,00%	2,05	0,307	-0,0414	0	1	0	0	2	1555,7142	66	79
									SYELQESNVR	R	L	95,00%	2,5	0,267	2,08	0	1	0	0	2	1224,5859	84	93
Phosphoglycerate kinase 1 (EC 2.7.2.3) - Mus musculus (Mouse)	PGK1_MOUSE	44533,1	100,00%	3	3	4	0,19%	8,39%	DVLFLK	K	D	95,00%	1,68	0	1,4	2	0	0	0	2	734,4454	92	97
									VLNNMEIGTSLYDEEGAK	K	I	95,00%	2,58	0,37	0	0	1	0	0	2	1998,9331	247	264
									VLPGVDALSNV	K	-	95,00%	2,76	0,212	1,4	0	1	0	0	2	1083,6051	407	417
Aspartate aminotransferase, cytoplasmic (EC 2.6.1.1) (Transaminase A) (Glutamate	AATC_RAT	46411,5	100,00%	4	5	5	0,28%	13,10%	ITWSNPPAQGAR	R	I	95,00%	3,01	0,308	1,17	0	1	0	0	2	1297,6654	294	305
									LIADFRDDPDPR	K	K	95,00%	0	0	3,09	0	0	1	0	2	1429,708	21	32
									SCASQLVLCDNSPALR	R	E	95,00%	2,26	0,254	-1	0	2	0	0	2	1687,8439	82	97
									VGGVQSLGGTGALR	R	I	95,00%	3,4	0,378	4,64	0	1	0	0	2	1271,7074	101	114
		100,00%	2	2	3	0,17%	6,30%	LIADFRDDPDPR	K	K	95,00%	3,31	0,245	0	0	0	1	0	2	1429,708	21	32
									VGGVQSLGGTGALR	R	I	95,00%	2,41	0,293	0	0	2	0	0	2	1271,7074	101	114
Creatine kinase M-type (EC 2.7.3.2) (Creatine kinase M chain) (M-CK) - Mus musculu	KCRM_MOUSE,KCRM_RAT	43027,6	100,00%	1	2	3	0,16%	3,68%	GGDDLDPNYVLSSR	K	V	95,00%	2,88	0,414	-0,505	0	3	0	0	2	1507,7031	117	130
Long-chain specific acyl-CoA dehydrogenase, mitochondrial precursor (EC 1.3.99.13)	ACADL_RAT	47855,8	100,00%	5	8	8	0,34%	13,70%	AQDTAELFFEDVR	K	L	95,00%	3,96	0,433	-0,869	0	1	0	0	2	1540,7285	255	267
									IFSSEHDIFR	R	E	95,00%	2,42	0,342	2,36	0	1	0	0	2	1250,6169	52	61
									LPASALLGEENK	R	G	95,00%	3,73	0,323	3,54	0	4	0	0	2	1241,6743	268	279
									SGSWILNGSK	R	V	95,00%	0	0	2,55	0	1	0	0	2	1163,5698	191	201
									VQPIYGGTNEIMK	R	E	95,00%	2,51	0,432	0	0	1	0	0	2	1465,7363	407	419
		100,00%	2	5	6	0,26%	5,12%	IFSSEHDIFR	R	E	95,00%	2,53	0,251	0	0	1	0	0	2	1250,6169	52	61
									LPASALLGEENK	R	G	95,00%	3,5	0,339	0	0	5	0	0	2	1241,6743	268	279
Serum albumin precursor (Allergen Equ c 3) - Equus caballus (Horse)	ALBU_HORSE	68581,9	100,00%	6	6	7	0,35%	9,56%	APQVSTPTLVEIGR	K	T	95,00%	2,27	0,409	-1,42	0	2	0	0	2	1467,8174	438	451
									CCTDSLAER	K	R	95,00%	2,16	0,308	3,15	0	1	0	0	2	1111,4514	499	507
									LPCSENHLALALNR	R	L	95,00%	2,69	0,315	0	0	1	0	0	2	1607,8329	469	482
									QIKKQSALAELVK	K	H	95,00%	0	0	4,13	0	0	1	0	2	1438,8636	545	557
									QSALAELVK	K	H	95,00%	1,91	0,166	2,26	0	1	0	0	2	958,5574	549	557
									TYEATLEK	K	C	95,00%	1,59	0,282	1,75	1	0	0	0	2	954,4784	375	382
Macrophage-capping protein (Actin-regulatory protein CAP-G) - Rattus norvegicus (R	CAPG_RAT	38781,7	99,10%	2	3	3	0,16%	6,59%	TTSGTTPAAIR	K	K	95,00%	1,95	0,0501	1,13	0	1	0	0	2	1075,5749	128	138
									VSDATGQMNLTK	K	V	95,00%	3,11	0,241	1,1	0	2	0	0	2	1280,6157	255	266
Aldose reductase (EC 1.1.1.21) (AR) (Aldehyde reductase) - Rattus norvegicus (Rat)	ALDR_RAT	35779,7	100,00%	3	3	3	0,16%	7,91%	EVGVALQEK	K	L	95,00%	1,91	0,163	3,38	0	1	0	0	2	972,5367	54	62
									TTAQVLIR	K	F	95,00%	2,8	0,235	4,05	0	1	0	0	2	901,5472	244	251
									VAIDMGYR	K	H	95,00%	2,02	0,194	3,48	0	1	0	0	2	940,4563	34	41
		100,00%	2	2	2	0,10%	5,38%	EVGVALQEK	K	L	95,00%	2,17	0,249	0	0	1	0	0	2	972,5367	54	62
									TTAQVLIR	K	F	95,00%	3,04	0,12	0	0	1	0	0	2	901,5472	244	251
Glyceraldehyde-3-phosphate dehydrogenase (EC 1.2.1.12) (GAPDH) - Columba livia	G3P_COLLI	35748,9	100,00%	2	2	2	0,10%	8,11%	GAAQNIIPASTGAAK	R	A	95,00%	3,09	0,154	0,569	0	1	0	0	2	1369,7441	199	213
									VVDLMVHMASKE	R	-	95,00%	2,56	0,232	0	0	1	0	0	2	1390,671	322	333
Triosephosphate isomerase (EC 5.3.1.1) (TIM) (Triose-phosphate isomerase) - Rattu	TPIS_RAT	26830,7	100,00%	3	4	4	0,25%	16,50%	CNVSEGVAQCTR	K	I	95,00%	1,94	0,264	0	0	1	0	0	2	1380,6001	195	206
									HIFGESDELIGQK	R	V	95,00%	2,51	0,296	-0,748	0	1	1	0	2	1472,7388	101	113
									VTNGAFTGEISPGMIK	K	D	95,00%	2,23	0,263	0	0	1	0	0	2	1637,8212	70	85

ATP synthase D chain, mitochondrial (EC 3.6.3.14) - Rattus norvegicus (Rat)	ATP5H_RAT	18746	100,00%	3	4	5	0,25%	24,20%	ANVDKPGLVDDFK	R	N	95,00%	2,78	0,329	-0,74	0	1	1	0	2	1417,7329	59	71
									NCAQFVTGSQAR	K	V	95,00%	3,05	0,262	-0,875	0	2	0	0	2	1338,6224	100	111
									YTALVDAEEKEDVK	K	N	95,00%	3,18	0,292	0	0	1	0	0	2	1609,7963	86	99
			99,80%	2	2	2	0,10%	16,80%	ANVDKPGLVDDFK	R	N	95,00%	2,98	0,338	0	0	1	0	0	2	1417,7329	59	71
									YTALVDAEEKEDVK	K	N	95,00%	3,52	0,323	0	0	1	0	0	2	1609,7963	86	99
Myosin regulatory light chain 2, ventricular/cardiac muscle isoform (MLC-2) (MLC-2v/	MLRV_BOVIN	18963,3	100,00%	5	6	6	0,32%	24,10%	DTFAALGR	R	V	95,00%	1,72	0,0754	1,19	1	0	0	0	2	850,4424	51	58
									EAFTIMDQNR	K	D	95,00%	2,78	0,133	0,215	0	1	0	0	2	1240,5632	31	40
									EMLTTQAER	K	F	95,00%	2	0,101	1,16	0	1	0	0	2	1094,5153	121	129
									NLVHIITHGEEK	K	-	95,00%	2,73	0,215	-0,204	0	2	0	0	2	1389,7493	154	165
									NLVHIITHGEEKD	K	-	95,00%	2,87	0,384	0	0	1	0	0	2	1504,7762	154	166
T-complex protein 1 subunit zeta (TCP-1-zeta) (CCT-zeta) (CCT-zeta-1) (Tcp20) (HT	TCPZ_HUMAN,TCPZ_PONPY	58007,3	100,00%	3	4	4	0,19%	5,46%	ALQFLEEVK	K	V	95,00%	1,91	0	1,89	0	1	0	0	2	1076,5994	130	138
									MLVSGAGDIK	K	L	95,00%	2,65	0,207	3,02	0	1	0	0	2	1006,5244	46	55
									TEVNSGFPYK	K	S	95,00%	1,82	0,0381	2,11	0	2	0	0	2	1191,5686	242	251
Myosin regulatory light chain 2A, cardiac muscle isoform (G2) (MLC-2A) - Gallus galli	MLRA_CHICK	18688,1	99,80%	2	5	18	3,49%	9,09%	GADPEETILNAFK	K	V	95,00%	3,84	0,21	7,2	0	8	0	0	2	1404,7013	92	104
									LKGADPEETILNAFK	K	V	95,00%	4	0,331	8,52	0	4	6	0	2	1645,8804	90	104
Tropomyosin alpha-4 chain (Tropomyosin-4) (TM-4) - Rattus norvegicus (Rat)	TPM4_RAT	28492,4	100,00%	4	7	8	1,39%	17,70%	IQLVEEELDRAQER	R	L	95,00%	1,88	0,0703	6,51	0	0	1	0	2	1727,8929	56	69
									LVILEGELER	K	A	95,00%	2,68	0,292	4,92	0	1	0	0	2	1170,6736	133	142
									LVILEGELERAEER	K	A	95,00%	3,77	0,313	5,3	0	1	3	0	2	1655,897	133	146
									SSDLEEELKNVTNNLK	K	S	95,00%	4,75	0,281	6,6	0	2	0	0	2	1832,9242	154	169
Actin-1 - Aedes aegypti (Yellowfever mosquito)	ACT1_AEDAE	41773,6	100,00%	5	9	24	1,89%	26,60%	DLTDYLMK	R	I	95,00%	2,64	0,131	2,54	3	3	0	0	2	998,4871	185	192
									DLYANTVLSGGTTMYPGIADR	K	M	95,00%	5,28	0,312	7	0	1	1	0	2	2231,0659	293	313
									IWHHTFYNELR	K	V	95,00%	2,22	0,0191	3	0	0	3	0	2	1515,7496	86	96
									KDLYANTVLSGGTTMYPGIADR	R	M	95,00%	4,96	0,219	10,2	0	0	1	0	2	2359,1609	292	313
									LDLAGRDLTDYLMK	R	I	95,00%	2,31	0	7,46	0	0	2	0	2	1639,8369	179	192
									SYELPDGQVITIGNER	K	F	95,00%	3,83	0,318	6,08	0	15	4	0	2	1790,8926	240	255
									VAPEEHPVLLTEAPLNPK	R	A	95,00%	4,52	0,285	1,68	0	6	13	0	2	1954,0653	97	114
									VAPEEHPVLLTEAPLNPKANR	R	E	95,00%	3,49	0,086	2,96	0	0	1	0	2	2295,2463	97	117
									YPNEHGIITNWDDMEK	K	I	95,00%	2,42	-0,0819	3,52	0	1	0	0	2	1961,8706	70	85
Actin, muscle 2/4/4A - Halocynthia roretzi (Sea squirt)	ACT2_HALRO	41997	100,00%	9	17	45	3,54%	28,30%	DLTDYLMK	R	I	95,00%	2,64	0,131	2,54	3	3	0	0	2	998,4871	187	194
									DLYANNVLSGGTTMYPGIADR	K	M	95,00%	4,87	0,248	5,68	0	1	1	0	2	2244,061	295	315
									GYSFVTTAER	R	E	95,00%	3,05	0,317	4,68	0	2	0	0	2	1130,5482	200	209
									IWHHTFYNLR	K	V	95,00%	2,22	0,0191	3	0	0	3	0	2	1515,7496	88	98
									KDLYANNVLSGGTTMYPGIADR	R	M	95,00%	5,2	0,158	2,85	0	0	2	0	2	2372,156	294	315
									LDLAGRDLTDYLMK	R	I	95,00%	2,31	0	7,46	0	0	2	0	2	1639,8369	181	194
									SYELPDGQVITIGNER	K	F	95,00%	3,83	0,318	6,08	0	15	4	0	2	1790,8926	242	257
									VAPEHPTLLTEAPLNPK	R	A	95,00%	3,84	0,18	5,3	0	4	4	0	2	1956,0447	99	116
									YPIEHGIITNWDDMEK	K	I	95,00%	3,87	0,116	2,75	0	0	1	0	2	1976,9066	72	87
Tropomyosin-1 alpha chain (Alpha-tropomyosin) - Homo sapiens (Human)	TPM1_HUMAN	32692	100,00%	9	16	42	5,10%	33,80%	CAELEEELK	K	T	95,00%	0	0	3,52	1	5	0	0	2	1103,4933	190	198
									CAELEEELKTVTNNLK	K	S	95,00%	3,43	0,334	6,11	0	0	3	0	2	1890,9484	190	205
									GTEDELDKYSEALKDAQEK	K	L	95,00%	4,3	0,137	7,42	0	0	3	0	2	2169,02	52	70
									IQLVEEELDR	R	A	95,00%	2,79	0,155	4,16	0	5	0	0	2	1243,6536	92	101
									IQLVEEELDRAQER	R	L	95,00%	2,15	0,0281	4,15	0	0	1	0	2	1727,8929	92	105
									LVIESDLERAEER	K	A	95,00%	1,88	0,0172	3,59	0	0	1	0	2	1671,8918	169	182
									MEIQEIQLK	K	E	95,00%	2,72	0,0549	5	0	1	0	0	2	1131,6086	141	149
									QLEDELVSLQK	K	K	95,00%	0	0	4,11	1	11	0	0	2	1284,669	38	48
									SIDDLEDELYAQK	K	L	95,00%	4,67	0,428	8,26	0	6	4	0	2	1538,7228	252	264
Vimentin - Bos taurus (Bovine)	VIME_BOVIN	53710,8	100,00%	2	2	4	0,42%	4,72%	ILLAELEQLK	K	G	95,00%	3,34	0,222	5,52	0	3	0	0	2	1169,7148	130	139
									VESLQEEIAFLK	K	K	95,00%	3,19	0,192	6,85	0	1	0	0	2	1405,7581	224	235
Vimentin - Bos taurus (Bovine)	VIME_BOVIN	53710,8	100,00%	2	2	2	0,21%	4,51%	ILLAELEQLK	K	G	95,00%	3,51	0,209	6,19	0	1	0	0	2	1169,7148	130	139
									MALDIEIATYR	K	K	95,00%	3,44	0,276	6,16	0	1	0	0	2	1311,662	391	401
ATP synthase subunit beta, mitochondrial precursor (EC 3.6.3.14) - Homo sapiens (H	ATPB_HUMAN	56542,5	100,00%	8	14	27	4,86%	22,90%	AIAELGIYPAVDPLDSTSR	R	I	95,00%	3,15	0,0584	2,47	0	1	0	0	2	1988,0343	388	406
									EGNDLYHEMIESGVINLK	R	D	95,00%	3,42	0	6,3	0	0	2	0	2	2076,9912	242	259
									FTQAGSEVSALLGR	R	I	95,00%	3,67	0,279	8,22	0	4	2	0	2	1435,7545	311	324
									LVLEVAQHLGESTVR	R	T	95,00%	4,79	0,53	9,75	0	4	5	0	2	1650,918	95	109
									TVLIMELINNVAK	K	A	95,00%	4,19	0,335	8,96	0	3	0	0	2	1473,8351	213	225
									VALTGLTVAEYFR	R	D	95,00%	3,97	0,077	8,13	0	1	0	0	2	1439,7899	282	294
									VLDSGAPIKIPVGPETLGR	K	I	95,00%	4,67	0,375	16	0	0	2	0	2	1919,097	125	143
									VVDLLAPYAK	K	G	95,00%	2,62	0,0835	4,37	0	3	0	0	2	1088,6357	189	198
ATP synthase subunit beta, mitochondrial precursor (EC 3.6.3.14) - Homo sapiens (H	ATPB_HUMAN	56542,5	100,00%	10	16	37	12,90%	29,10%	AIAELGIYPAVDPLDSTSR	R	I	95,00%	3,15	0,0598	8,28	0	1	0	0	2	1988,0343	388	406
									EGNDLYHEMIESGVINLK	R	D	95,00%	0	0	5,19	0	0	1	0	2	2076,9912	242	259
									FTQAGSEVSALLGR	R	I	95,00%	4,36	0,24	9,7	0	4	2	0	2	1435,7545	311	324
									IMNVIGEPIDER	R	G	95,00%	3,07	0,0891	5,54	0	2	0	0	2	1385,7101	144	155
									IPSAVGYQPTLATDMGTMQER	R	I	95,00%	6,72	0,368	11,7	0	0	1	0	2	2298,0749	325	345
									LVLEVAQHLGESTVR	R	T	95,00%	4,63	0,466	10,5	0	5	7	0	2	1650,918	95	109
									TVLIMELINNVAK	K	A	95,00%	4,7	0,281	8,96	0	3	0	0	2	1457,8402	213	225
									VALTGLTVAEYFR	R	D	95,00%	3,86	0,0124	6,54	0	0	1	0	2	1439,7899	282	294
									VLDSGAPIKIPVGPETLGR	K	I	95,00%	2,35	0,0937	5	0	1	3	0	2	1919,097	125	143
									VVDLLAPYAK	K	G	95,00%	2,26	0,171	2,64	0	6	0	0	2	1088,6357	189	198
Vimentin (Fragment) - Cricetulus griseus (Chinese hamster)	VIME_CRIGR	51831,8	100,00%	13	19	51	7,66%	22,50%	EEAESTLQSFR	R	Q	95,00%	1,95	0	2,92	0	1	0	0	2	1296,6072	179	189
									ETNLESLPLVDTHSK	R	R	95,00%	0	0	6,92	0	1	0	0	2	1664,8496	407	421
									ETNLESLPLVDTHSKR	R	T	95,00%	0	0	3,62	0	0	1	0	2	1838,9613	407	422
									ILLAELEQLK	K	G	95,00%	2,92	0,173	4,92	0	15	0	0	2	1169,7148	112	121
									ILLAELEQLKGQGK	K	S	95,00%	4,73	0,327	6,62	0	4	3	0	2	1539,9114	112	125
									ISLPLPNFSSLNLR	R	E	95,00%	2,82	0,253	3,34	0	1	0	0	2	1570,8957	393	406
									KVESLQEEIAFLK	R	K	95,00%	5,16	0,304	9,1	0	3	4	0	2	1533,8529	205	217
									KVESLQEEIAFLKK	R	L	95,00%	5,09	0,204	8,38	0	0	6	0	2	1661,9479	205	218
									MALDIEIATYR	K	K	95,00%	3,95	0,383	6,92	0	3	0	0	2	1311,662	373	383
									QVQSLTCEVDALK	R	G	95,00%	0	0	4,66	0	4	0	0	2	1473,7262	304	316
									QVQSLTCEVDALKGTNESLER	R	Q	95,00%	2,94	0,311	2,85	0	0	2	0	2	2377,167	304	324
									VESLQEEIAFLK	K	K	95,00%	4,3	0,35	7,55	0	2	0	0	2	1405,7581	206	217
									VESLQEEIAFLKK	K	L	95,00%	2,32	0,229	0,42	0	0	1	0	2	1533,853	206	218
Calreticulin precursor (CRP55) (Calregulin) (HACBP) (ERp60) (CALBP) (Calcium-bindi	CALR_RAT	47979	100,00%	8	14	19	1,76%	17,80%	DEDEDEDEKEEDEEDEEDATGQAK	R	D	95,00%	4,61	0,418	2,8	0	0	1	0	2	2554,9556	392	413
									DPDAAKPEDWDER	K	A	95,00%	0	0	3,82	0	0	2	0	2	1543,6667	210	222
									EQFLDGDAWTNR	K	W	95,00%	2,83	0,468	8,19	0	3	0	0	2	1451,6556	25	36
									FVLSGK	K	F	95,00%	1,89	0,201	1,96	1	0	0	0	2	737,4197	49	55
									IKDPDAAKPEDWDER	K	A	95,00%	3,64	0,375	4,17	0	2	5	0	2	1784,846	208	222
									KVHVIFNYK	K	G	95,00%	2,21	0,343	2,29	0	1	0	0	2	1147,6628	143	151
									LPGGLDQK	K	D	95,00%	2,37	0,257	3,7	0	3	0	0	2	974,5313	112	120
									VHVIFNYK	K	G	95,00%	1,83	0,286	2,26	0	1	0	0	2	1019,5678	144	151
Alpha-1-antiproteinase 2 precursor (Alpha-1-antitrypsin 2) (Alpha-1-proteinase inhib	A1AT2_HORSE	46925,8	100,00%	6	8	11	0,72%	14,00%	AVLTIDEK	K	G	95,00%	2,19	0,165	1,96	2	0	0	0	2	888,5043	363	370
									DTVLALVNYIFFK	K	G	95,00%	3,18	0,283	1,48	0	1	0	0	2	1542,8572	206	218
									IAPNLADFAFSLYR	K	H	95,00%	4,61	0,502	4,28	0	4	0	0	2	1597,838	53	66
									LLDKFLEDVK	K	K	95,00%	0	0	4,36	0	1	0	0	2	1219,6941	153	162
									SPLFVGK	K	V	95,00%	1,54	0,028	1,28	2	0	0	0	2	747,4406	408	414
									SPLFVGKVVDPTQK	K	-	95,00%	2,5	0,316	0,432	0	0	1	0	2	1514,8586	408	421
Alpha-1-antiproteinase 2 precursor (Alpha-1-antitrypsin 2) (Alpha-1-proteinase inhib	A1AT2_HORSE	46925,8	100,00%	5	6	6	0,58%	13,30%	HSSFVNVNLPK	R	L	95,00%	0	0	5,01	0	2	0	0	2	1264,6803	307	317
									IAPNLADFAFSLYR	K	H	95,00%	2,26	0,351	1,07	0	1	0	0	2	1597,838	53	66
									LQHLEDTLTK	K	G	95,00%	2,89	0,284	4,55	0	1	0	0	2	1197,6482	287	296
									QADLSGITEEVPLTVSK	R	A	95,00%	2,64	0,336	4,27	0	1	0	0	2	1786,9441	342	358
									QADLSGITEEVPLTVSKALHK	R	A	95,00%	0	0	4	0	0	1	0	2	2236,219	342	362

Protein disulfide-isomerase A3 precursor (EC 5.3.4.1) (Disulfide isomerase ER-60) (EPDIA3_RAT	56607,5	100,00%	12	26	32	2,72%	30,30%	DGEEAGAYDGPR	R	T	95,00%	2,37	0,327	2,8	0	5	0	0	2	1236,5135	108	119
								EATNPPIIQEEKPK	R	K	95,00%	2,85	0,5	6,1	0	5	0	0	2	1593,8492	483	496
								ELNDFISYLQR	R	E	95,00%	2,06	0,267	1,19	0	3	0	0	2	1397,7065	472	482
								FLQEYFDGNLK	R	R	95,00%	3,31	0,267	6,82	0	1	0	0	2	1373,6742	352	362
								FLQEYFDGNLKR	R	Y	95,00%	3,34	0,287	4,75	0	1	0	0	2	1529,7753	352	363
								KFISDKDASVVGFFR	K	D	95,00%	0	0	4,48	0	0	1	0	2	1715,912	147	161
								LAPEYEAAATR	R	L	95,00%	2,63	0,275	5,32	0	4	0	0	2	1191,6011	63	73
								MDATANDVPSPYEVK	K	G	95,00%	4,28	0,405	8,15	0	3	0	0	2	1652,7478	434	448
								SEPIPETNEGPVK	K	V	95,00%	1,74	0,0762	3,14	0	1	0	0	2	1396,6963	367	379
								TADGIVSHLK	R	K	95,00%	2,81	0,352	4,72	0	1	0	0	2	1040,5742	120	129
								TFSHELSDFGLESTTGEIPVVAIR	K	T	95,00%	2,11	0,0827	7,35	0	0	2	0	2	2605,3149	306	329
								VVVAESFDDIVNAEDK	K	D	95,00%	5,24	0,497	9,8	0	4	1	0	2	1749,8546	380	395
Alpha-enolase (EC 4.2.1.11) (2-phospho-D-glycerate hydro-lyase) (Non-neural enola	ENOA_RAT	47111	100,00%	15	54	88	2,68%	44,50%	AAVPSGASTGIYEALELR	R	D	95,00%	4,72	0,501	4,57	0	8	1	0	2	1804,9447	33	50
								AGKYDLDFKSPDDASR	R	Y	95,00%	4,77	0,309	8	0	2	1	0	2	1784,8458	254	269
								DATNVGDEGGFAPNILENK	K	E	95,00%	4,06	0,136	8,51	0	4	0	0	2	1960,9254	203	221
								DATNVGDEGGFAPNILENKEALELLK	K	S	95,00%	4,21	0,428	3,25	0	0	1	0	2	2757,3945	203	228
								GNPTVEVDLVTAK	R	G	95,00%	2,4	0,0539	3,96	0	7	0	0	2	1406,7169	16	28
								HIADLAGNPEVILPVPAFNVINGGSHAGNK	R	L	95,00%	7,22	0,024	5,51	0	0	4	0	2	3021,5911	133	162
								IDQLMIEMDGTENK	K	S	95,00%	3,82	0	2,17	0	7	0	0	2	1652,7515	90	103
								IGAEVYHNLK	R	N	95,00%	2,96	0,19	1,39	0	3	0	0	2	1143,6163	184	193
								LAMQEFMILPVGASSFR	K	E	95,00%	3,44	0,0674	3,1	0	10	2	0	2	1896,9717	163	179
								LAQSNGWGVMVSHR	K	S	95,00%	2,6	0	5,41	0	4	1	0	2	1541,7645	359	372
								LNVVEQEK	K	I	95,00%	2,23	0,0166	4,18	0	8	0	0	2	958,5209	82	89
								LNVVEQEKIDQLMIEMDGTENK	K	S	95,00%	6,11	0,418	3,85	0	0	1	0	2	2608,249	82	103
								VNQIGSVTESLQACK	K	L	95,00%	3,92	0,288	4,2	0	9	1	0	2	1633,822	344	358
								YDLDFKSPDDASR	K	Y	95,00%	3,95	0,179	3,7	0	3	0	0	2	1528,6923	257	269
								YITPDQLADLYK	R	S	95,00%	2,42	0,12	5,24	0	11	0	0	2	1439,7425	270	281
Laminin subunit alpha-1 precursor (Laminin A chain) - Mus musculus (Mouse)	LAMA1_MOUSE	338149,2	100,00%	9	10	11	0,65%	3,79%	ADNEVICTSYYSK	R	L	95,00%	3,14	0,337	1,36	0	1	0	0	2	1549,6844	183	195
								AEGLSLQPYEEYFNVVR	R	L	95,00%	3,78	0,426	3,59	0	1	0	0	2	2013,9919	630	646
								ALLHAPTGSYSDQGEHSISLVR	K	N	95,00%	3,16	0,242	2,59	0	0	2	0	2	2338,1792	2576	2597
								DLIYVGGLPHSK	K	A	95,00%	2,43	0,342	0,658	0	1	0	0	2	1298,7111	2440	2451
								ITATYQPR	R	A	95,00%	1,71	0,103	2,42	0	2	0	0	2	949,5108	2969	2976
								LYLGGLPSHYR	K	A	95,00%	2,03	0,168	1,77	0	1	0	0	2	1275,6851	2845	2855
								NGVLLGISSAK	K	V	95,00%	1,9	0,202	1,82	0	1	0	0	2	1058,6211	2935	2945
								TLNADLMTLSHR	R	D	95,00%	0	0	2,96	0	1	0	0	2	1387,7006	240	251
								VSHPALLSDGK	K	W	95,00%	2,07	0,294	0,854	0	1	0	0	2	1123,6113	2795	2805
Elongation factor 2 (EF-2) - Cricetulus griseus (Chinese hamster)	EF2_CRIGR	95380	100,00%	4	8	10	0,59%	5,48%	CLYASVLTAQPR	R	L	95,00%	3,1	0,424	4,62	0	5	0	0	2	1378,7154	728	739
								ETVSEESNVLCLSK	R	S	95,00%	3,99	0,463	5,66	0	2	0	0	2	1594,7634	581	594
								IMGPNYTPGK	R	K	95,00%	2,35	0,25	1,35	0	1	0	0	2	1093,5354	429	438
								VFSGVVSTGLK	R	V	95,00%	3,39	0,36	7,27	0	2	0	0	2	1093,6257	416	426
Serotransferrin precursor (Transferrin) (Siderophilin) (Beta-1 metal-binding globulin)	TRFE_HORSE	78076,6	100,00%	37	93	166	3,92%	54,80%	AACVCQELHNQQASYGK	K	N	95,00%	5,9	0,582	8,04	0	1	1	0	2	1963,8756	621	637
								APNHAVVSR	R	K	95,00%	1,85	0,401	2,4	0	2	0	0	2	950,5171	609	617
								AVSNFFAGSCVPCADR	K	T	95,00%	4,51	0,497	5,52	0	16	0	0	2	1757,774	165	180
								CACSNHEPYFGYSGAFK	K	C	95,00%	4,36	0,537	5,28	0	3	1	0	2	1994,8165	198	214
								CGLVPVLAENYETR	K	S	95,00%	0	0	5,27	0	9	0	0	2	1603,7793	423	436
								CLADGAGDVAFVK	K	H	95,00%	0	0	3,41	0	16	0	0	2	1305,6152	215	227
								CLVEKGDVAFVK	R	H	95,00%	3,03	0	3,3	0	5	0	0	2	1364,725	550	561
								DCYLASIPSHAVVAR	K	S	95,00%	3,69	0,396	3,42	0	2	0	0	2	1658,8324	261	275
								DDTQCLAKQPTTTYK	R	T	95,00%	5,28	0,492	5,03	0	6	0	0	2	1868,8705	660	675
								DEYQLLCR	R	D	95,00%	2,39	0,177	0,77	0	1	0	0	2	1096,51	242	249
								DFHLFSSPHGK	K	D	95,00%	2,97	0,386	1,17	0	1	0	0	2	1271,6173	302	312
								DLKSENFK	K	L	95,00%	1,98	0,145	2,5	0	2	0	0	2	980,5054	580	587
								DLLFKDSALGFLR	K	I	95,00%	3,19	0,0742	3,41	0	2	0	0	2	1494,8323	313	325
								DLLFRDDTQCLANLQPTTTYK	K	T	95,00%	2,79	0,332	2,68	0	0	1	0	2	2513,2349	655	675
								EDIRPEVPKDECK	R	K	95,00%	1,88	0,277	0,041	0	3	0	0	2	1614,78	349	361
								FCLFQSATK	K	D	95,00%	2,48	0,235	3,68	0	3	0	0	2	1101,5404	646	654
								GDVAFVK	K	H	95,00%	1,83	0,0792	2,02	1	0	0	0	2	735,4042	555	561
								HQTVFQNTDGRNPDDWAK	K	D	95,00%	3,13	0,398	3,46	0	3	2	0	2	2110,9544	562	579
								KNSNFQLNQLQGK	K	K	95,00%	2,47	0,124	2,06	0	1	0	0	2	1518,803	119	131
								KSVDEYKDCYLASIPSHAVVAR	R	S	95,00%	5,18	0,421	0,886	0	0	2	0	2	2508,2556	254	275
								LLCPDGTR	K	K	95,00%	1,8	0,149	2,57	0	3	0	0	2	931,4673	588	595
								LLEACTFHR	R	-	95,00%	2,47	0,2	0,377	0	2	0	0	2	1146,5731	697	705
								LLEACTFHRV	R	-	95,00%	1,81	0,192	1,7	0	3	0	0	2	1245,6415	697	706
								NGSHCPDKFCLFQSATK	K	D	95,00%	3,26	0,43	2,5	0	0	1	0	2	1996,9011	638	654
								NSNFQLNQLQGK	K	K	95,00%	3,73	0,321	1,39	0	9	0	0	2	1390,708	120	131
								RTSYLECIK	K	A	95,00%	2,3	0,117	2,89	0	4	0	0	2	1169,599	58	66
								SAGWNIPIGLLYWQLPEPR	R	E	95,00%	4,97	0,475	6,82	0	3	1	0	2	2210,1765	141	159
								SIVPAPPLVACVK	K	R	95,00%	2,46	0,356	4,24	0	5	0	0	2	1350,7821	45	57
								SKDFHLFSSPHGK	K	D	95,00%	3,85	0,433	4,55	0	3	0	0	2	1486,7445	300	312
								SSSDPDLTWNSLK	K	G	95,00%	3,56	0,38	3,82	0	8	0	0	2	1449,6863	457	469
								SVDEYKDCYLASIPSHAVVAR	K	S	95,00%	6,29	0,503	4,89	0	0	6	0	2	2380,1606	255	275
								SVDGKEDLIWGLLNQAQEHFGTEK	R	S	95,00%	3,97	0,329	3,16	0	0	1	0	2	2714,3428	276	299
								TAGWNIPMGLLYSEIK	R	H	95,00%	2,74	0,118	3,03	0	2	0	0	2	1792,931	481	496
								TAVPNLCQLCVGK	R	G	95,00%	2,7	0,469	5,21	0	9	0	0	2	1459,7404	181	193
								TSYLECIK	R	A	95,00%	1,86	0,216	-0,255	2	2	0	0	2	1013,4979	59	66
								YLTAVANLR	K	Q	95,00%	1,7	0,228	1,08	0	11	0	0	2	1020,5842	682	690
								YYGYTGAFR	R	C	95,00%	1,74	0,316	-0,74	1	6	0	0	2	1097,5056	541	549
Malate dehydrogenase, cytoplasmic (EC 1.1.1.37) (Cytosolic malate dehydrogenase)	MDHC_MOUSE	36494,1	100,00%	5	10	14	1,96%	21,60%	DLDVAVLVGSMPR	K	R	95,00%	3,04	0,395	5,5	0	1	0	0	2	1387,7257	80	92
								FVEGLPINDFSR	K	E	95,00%	2,24	0,379	5,66	0	5	0	0	2	1393,7117	299	310
								GEFITTVQQR	K	G	95,00%	3,29	0,327	4,7	0	4	0	0	2	1178,6172	221	230
								NVIIWGNHSSTQYPDVNHAK	K	V	95,00%	0	0	6,42	0	0	2	0	2	2280,1162	180	199
								VIVVGNPANTNCLTASK	K	S	95,00%	4,51	0,528	12	0	2	0	0	2	1757,922	126	142
78 kDa glucose-regulated protein precursor (GRP 78) (Heat shock 70 kDa protein 5)	GRP78_HUMAN	72316,7	100,00%	6	10	13	2,39%	12,70%	DAGTIAGLNVMR	K	I	95,00%	3,19	0,332	5,96	0	2	0	0	2	1233,6263	186	197
								ITPSYVAFTPEGER	R	L	95,00%	3,63	0,526	2,05	0	5	0	0	2	1566,7806	61	74
								KKEIEEIVQPIISK	K	L	95,00%	3,29	0,119	5,19	0	0	2	0	2	1653,9795	620	633
								TFAPEEISAMVLTK	K	M	95,00%	2,95	0,0552	8	0	1	0	0	2	1552,7933	139	152
								TWNDPSVQQDIK	R	F	95,00%	3,54	0,322	5,7	0	1	0	0	2	1430,6918	102	113
								VTHAVVTVPAYFNDAQR	K	Q	95,00%	0	0	10,5	0	0	2	0	2	1887,9716	165	181
Tropomyosin beta chain (Tropomyosin 2) (Beta-tropomyosin) - Homo sapiens (Huma	TPM2_HUMAN	32833,7	100,00%	9	14	20	2,48%	23,20%	CKQLEEEQQALQK	R	K	95,00%	3,59	0,442	4,4	0	1	0	0	2	1631,8066	36	48
								CKQLEEEQQALQKK	R	L	95,00%	0	0	4,27	0	0	1	0	2	1759,9016	36	49
								IQLVEEELDR	R	A	95,00%	2,76	0,276	6,05	0	2	0	0	2	1243,6536	92	101
								KATDAEADVASLNR	K	R	95,00%	4,25	0,357	7,62	0	2	0	0	2	1460,7346	77	90
								LEEAEKAADESER	K	G	95,00%	0	0	4,52	0	0	1	0	2	1476,6819	113	125
								LVILEGELER	K	S	95,00%	2,87	0,21	4,4	0	4	0	0	2	1170,6736	169	178
								QLEEEQQALQK	K	K	95,00%	0	0	5,4	0	4	0	0	2	1326,6544	38	48
								RIQLVEEELDR	R	A	95,00%	2,96	0,206	4,25	0	2	0	0	2	1399,7546	91	101
								RIQLVEEELDRAQER	R	L	95,00%	3,78	0,404	1,39	0	0	3	0	2	1883,994	91	105
Desmin - Mesocricetus auratus (Golden hamster)	DESM_MESAU	53421,5	100,00%	20	43	53	8,56%	43,50%	ADVDAATLAR	R	I	95,00%	3,98	0,403	6,89	0	5	0	0	2	1002,522	212	221
								DGEVVSEATQQQHEVL	R	-	95,00%	3,58	0,453	4,6	0	4	0	0	2	1768,8356	454	469
								DNLIDDLQR	R	L	95,00%	2,41	0,283	4,09	0	2	0	0	2	1101,5543	180	188
								EEAENNLAAFR	R	A	95,00%	2,59	0,216	6,01	0	3	0	0	2	1263,5969	201	211
								EYQDLLNVK	R	M	95,00%	1,63	0,193	1,89	0	1	0	0	2	1121,5845	386	394
								FASEASGYQDNIAR	R	L	95,00%	4,66	0,529	8,08	0	3	0	0	2	1528,7031	355	368
								FASEASGYQDNIARLEEEIR	R	H	95,00%	2,6	0,278	5,03	0	0	1	0	2	2298,1001	355	374
								FLEQQNAALAAEVNR	R	L	95,00%	5,36	0,459	9,68	0	2	0	0	2	1673,861	127	141
								HQIQSYTCEIDALK	R	G	95,00%	4,09	0,45	6,14	0	1	5	0	2	1705,8223	325	338
								INLPIQTFSALNFR	R	E	95,00%	3,82	0,464	8,38	0	3	0	0	2	1633,9065	415	428
								LQEEIQLR	K	E	95,00%	2,44	0,148	3,5	0	3	0	0	2	1028,5742	193	200
								MALDVEIATYR	K	K	95,00%	3,43	0,472	6,14	0	4	0	0	2	1297,6464	395	405
								NISEAEEWYK	K	S	95,00%	3,27	0,334	4,13	0	3	0	0	2	1268,58	287	296
								QVEVLTNQR	R	A	95,00%	1,91	0,193	3,5	0	3	0	0	2	1086,5908	164	172
								TNEKVELQELNDR	R	F	95,00%	2,68	0,279	3,28	0	3	0	0	2	1587,798	105	117
								VAELYEEEMR	R	E	95,00%	3,22	0,452	4,72	0	2	0	0	2	1268,5834	150	159
								VAELYEEEMRELR	R	R	95,00%	1,98	0,269	-0,0414	0	0	1	0	2	1682,806	150	162
								VAELYEEEMRELRR	R	Q	95,00%	2,21	0,108	3,85	0	0	1	0	2	1838,9071	150	163
								VDVERDNLIDDLQR	R	L	95,00%	2,47	0,282	0,854	0	0	1	0	2	1699,8617	175	188
								VSDLTQAANKNNDALR	K	Q	95,00%	1,8	0	6,43	0	0	2	0	2	1729,8833	299	314

Vimentin (Fragment) - Cricetulus griseus (Chinese hamster)	VIME_CRIGR	51831,8	100,00%	27	64	87	4,56%	53,40%	DGQVINETSQHHDDLE	R	-	95,00%	3,2	0,266	3,7	0	3	0	0	2	1836,8002	433	448
									EEAESTLQSFR	R	Q	95,00%	2,44	0,453	5,41	0	4	0	0	2	1296,6072	179	189
									ETNLESLPLVDTHSK	R	R	95,00%	2,14	0,211	2,77	0	2	0	0	2	1682,8602	407	421
									EYQDLLNVK	R	M	95,00%	1,93	0,292	1,44	0	3	0	0	2	1121,5845	364	372
									FADLSEAANR	K	N	95,00%	2,2	0,312	2,52	0	5	0	0	2	1093,5278	277	286
									FADYIDK	R	V	95,00%	2,11	0,11	1,48	2	0	0	0	2	871,4202	96	102
									FADYIDKVR	R	F	95,00%	3,14	0,24	4,18	0	2	0	0	2	1126,5898	96	104
									ILLAELEQLK	K	G	95,00%	2,65	0,229	4,28	0	5	0	0	2	1169,7148	112	121
									ILLAELEQLKGQGK	K	S	95,00%	3,79	0,405	6,6	0	3	0	0	2	1539,9114	112	125
									ISLPLPNFSSLNLR	R	E	95,00%	2,03	0,295	1,89	0	5	0	0	2	1570,8957	393	406
									KVESLQEEIAFLK	R	K	95,00%	4,15	0,288	0,244	0	2	4	0	2	1533,8529	205	217
									KVESLQEEIAFLKK	R	L	95,00%	3,18	0,398	2,89	0	1	0	0	2	1661,9479	205	218
									LGDLYEEEMR	R	E	95,00%	3,22	0,464	5,32	0	4	0	0	2	1270,5627	128	137
									LQDEIQNMK	R	E	95,00%	2,12	0,149	2,47	0	1	0	0	2	1134,5466	347	355
									LQDEIQNMKEEMAR	R	H	95,00%	1,96	0	4,55	0	0	1	0	2	1766,8054	347	360
									LQEEMLQR	K	E	95,00%	2,57	0,0424	1,8	0	1	0	0	2	1062,5255	171	178
									LQEEMLQREEAESTLQSFR	K	Q	95,00%	3,24	0,308	6,82	0	0	1	0	2	2340,1143	171	189
									MALDIEIATYR	K	K	95,00%	3,7	0,429	3,77	0	1	0	0	2	1311,662	373	383
									NLQEAEEWYK	K	S	95,00%	2,68	0,224	4,89	0	5	0	0	2	1309,6066	265	274
									QDVDNASLAR	R	L	95,00%	2,71	0,385	6,07	0	7	0	0	2	1088,5337	190	199
									QVDQLTNDKAR	R	V	95,00%	0	0	4	0	2	0	0	2	1270,6394	142	152
									QVQSLTCEVDALK	R	G	95,00%	0	0	4,07	0	1	0	0	2	1473,7262	304	316
									QVQSLTCEVDALKGTNESLER	R	Q	95,00%	0	0	5,43	0	4	1	0	2	2360,1404	304	324
									SLYSSSPGGAYVTR	R	S	95,00%	2,95	0,356	11,2	0	8	0	0	2	1444,707	33	46
									TNEKVELQELNDR	R	F	95,00%	3,62	0,358	6,8	0	3	1	0	2	1587,798	83	95
									TVETRDGQVINETSQHHDDLE	K	-	95,00%	2,88	0,22	1,27	0	0	3	0	2	2423,1072	428	448
									VELQELNDR	K	F	95,00%	2,57	0,114	3,7	0	2	0	0	2	1115,5698	87	95
Vimentin (Fragment) - Cricetulus griseus (Chinese hamster)	VIME_CRIGR	51831,8	100,00%	21	46	60	5,95%	44,00%	DGQVINETSQHHDDLE	R	-	95,00%	3,55	0,345	4,25	0	4	1	0	2	1836,8002	433	448
									EEAESTLQSFR	R	Q	95,00%	2,46	0,289	2,18	0	1	0	0	2	1296,6072	179	189
									EEAESTLQSFRQDVDNASLAR	R	L	95,00%	0	0	7,08	0	0	1	0	2	2366,1221	179	199
									ETNLESLPLVDTHSK	R	R	95,00%	3,54	0,42	6,41	0	1	0	0	2	1682,8602	407	421
									EYQDLLNVK	R	M	95,00%	2,06	0,261	3,42	0	2	0	0	2	1121,5845	364	372
									FADLSEAANR	K	N	95,00%	3,05	0,147	5,28	0	4	0	0	2	1093,5278	277	286
									ILLAELEQLK	K	G	95,00%	3,61	0,217	4,24	0	2	0	0	2	1169,7148	112	121
									ILLAELEQLKGQGK	K	S	95,00%	2,39	0,126	4,14	0	0	3	0	2	1539,9114	112	125
									ISLPLPNFSSLNLR	R	E	95,00%	1,67	0,144	2,52	0	3	0	0	2	1570,8957	393	406
									KVESLQEEIAFLK	R	K	95,00%	5,21	0,369	8,35	0	1	2	0	2	1533,8529	205	217
									LGDLYEEEMR	R	E	95,00%	0	0	5,34	0	3	0	0	2	1254,5679	128	137
									LGDLYEEEMRELR	R	R	95,00%	1,99	0,166	4,33	0	0	2	0	2	1668,7905	128	140
									LIEGEESR	K	I	95,00%	2,54	0,122	3,55	0	2	0	0	2	932,4689	385	392
									MALDIEIATYR	K	K	95,00%	1,84	0	2,8	0	3	0	0	2	1311,662	373	383
									NLQEAEEWYK	K	S	95,00%	2,71	0,406	5,55	0	5	0	0	2	1309,6066	265	274
									QDVDNASLAR	R	L	95,00%	2,34	0,355	3,77	0	7	0	0	2	1088,5337	190	199
									QQYESVAAK	R	N	95,00%	0	0	3,46	0	2	0	0	2	1006,4845	256	264
									QVQSLTCEVDALK	R	G	95,00%	3,68	0,425	6	0	4	0	0	2	1490,7527	304	316
									QVQSLTCEVDALKGTNESLER	R	Q	95,00%	2,88	0,346	1,66	0	0	3	0	2	2377,167	304	324
									TNEKVELQELNDR	R	F	95,00%	2,5	0,198	0,444	0	0	3	0	2	1587,798	83	95
									VELQELNDR	K	F	95,00%	2,92	0,126	4,92	0	1	0	0	2	1115,5698	87	95

Online Table II: qPCR Primers and Probes

Target	5´-Primer	TaqMan Probe (5´-FAM, 3´-TAMRA)	3´-Primer
GAPDH	AAC TCC CTC AAG ATT GTC AGC AA	ATG GAC TGT GGT CAT GAG CCC TTC CA	CAG TCT TCT GAG TGG CAG TGA TG
CSQ2	TTT CTG ACG GAG ACG TTC AGG	TGG CTG CCT ACA GTA CGC TGG GAA C	TAG CAG GAC AGA GAG GGT GCA
α-cd actin	TGA TGC TCC CAG AGC TGT CTT	CCA CGC CAC CAG GGT GTC ATG GTA	GAT GCC TCG CTT GCT CTG AG
α-sk actin	TAT GAG GGT TAT GCC CTG CC	AAT CTC ACG TTC AGC TGT GGT CAC GAA GG	GCT TCT CTT TGA TGT CGC GC
α-MHC	ACA GAG TGC TTC GTG CCT GAT	ACA GTC ACC GTC TTG CCG TTT TCA GT	CGA ATT TCG GAG GGT TCT GC
β-MHC	GCC TAC AAG CGC CAG GCT	TTC ATT CAG GCC CTT GGC GCC AAT	CAT CCT TAG GGT TGG GTA GCA
bax	ATC CAC CAA GAA GCT GAG CG	ATC AGC AAT CAT CCT CTG CAG CTC CA	ACG GAA GAA GAC CTC TCG GG
Bcl-2	CCT GGT GGA CAA CAT CGC T	AAC GGA GGC TGG GAT GCC TTT GTG	AAT CAA ACA GAG GTC GCA TGC
VEGF-A	ACT GCT GTA CCT CCA CCA TGC	AAG TGG TCC CAG GCT GCA CCC A	AAG ATG TCC ACC AGG GTC TCA
Collagen α1(I)	TGG TCC TCA AGG TTT CCA AG	TGG CGG TTC AGG TCC AAT GG	TTA CCA GCT TCC CCA TCA TC
Collagen α1(III)	AAT GGT GGC TTT CAG TTC AGC T	TGG AAA GAA GTC TGA GGA AGG CCA GCT G	TGT AAT GTT CTG GGA GGC CC
MMP-2	CCGAGGACTATGACCGGGATAA	TCTGCCCCGAGACCGCTATGTCCA	CTTGTTGCCCAGGAAAGTGAAG
MMP-3	CCGTTTCCATCTCTCTCAAGATGA	AGATGGTATTCAATCCCTCTATGGACCTCC	CAGAGAGTTAGATTTGGTGGGTACCA
MMP-13	GGAAGACCCTCTTCTTCTCA	TCTGGTTAGCATCATCATAACTCCACACGT	TCATAGACAGCATCTACTTTGTC
MMP-14	GAACTTTGACACCGTGGCCAT	CAGAACCATCGCTCCTTGAAGACAAACATC	CCGTCCATCACTTGGTTATTCCT
TIMP-1	TCCTCTTGTTGCTATCATTGATAGCTT	TTCTGCAACTCGGACCTGGTTATAAGG	CGCTGGTATAAGGTGGTCTCGAT
TIMP-2	GCTGGACGTTGGAGGAAAGA	TCTCCTTCCGCCTTCCCTGCAATTAGA	GCACAATAAAGTCACAGAGGGTAAT

Online Figure I

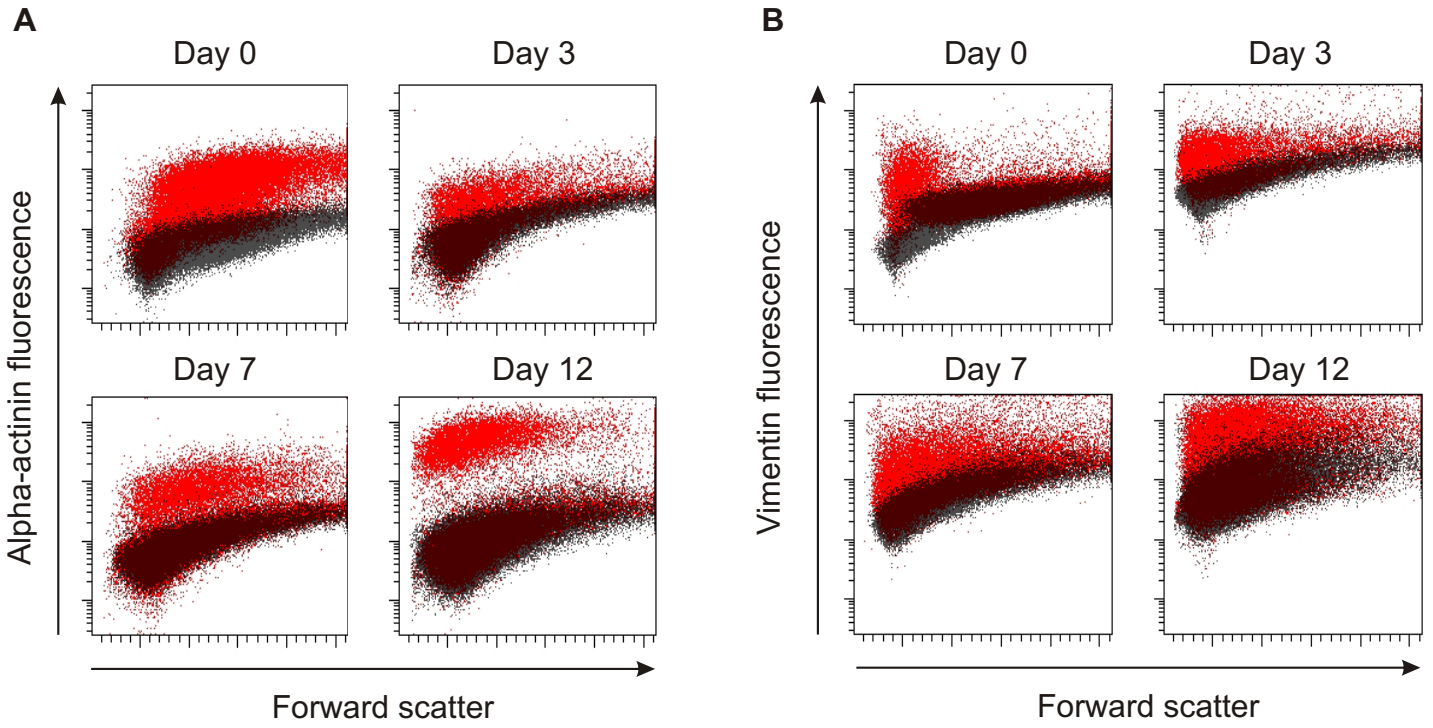

Online Figure I. Quantification of cardiomyocytes and fibroblasts during EHT culture by flow cytometry. Representative plots identify distinct a-actinin- (**A**) and vimentin-positive cell populations (**B**) at the indicated days of EHT culture. Panels resemble overlays of individual dot plots: in red cell pools labeled for actinin (**A**) or vimentin (**B**); in grey cell pools exposed to secondary antibody only.

Online Figure II

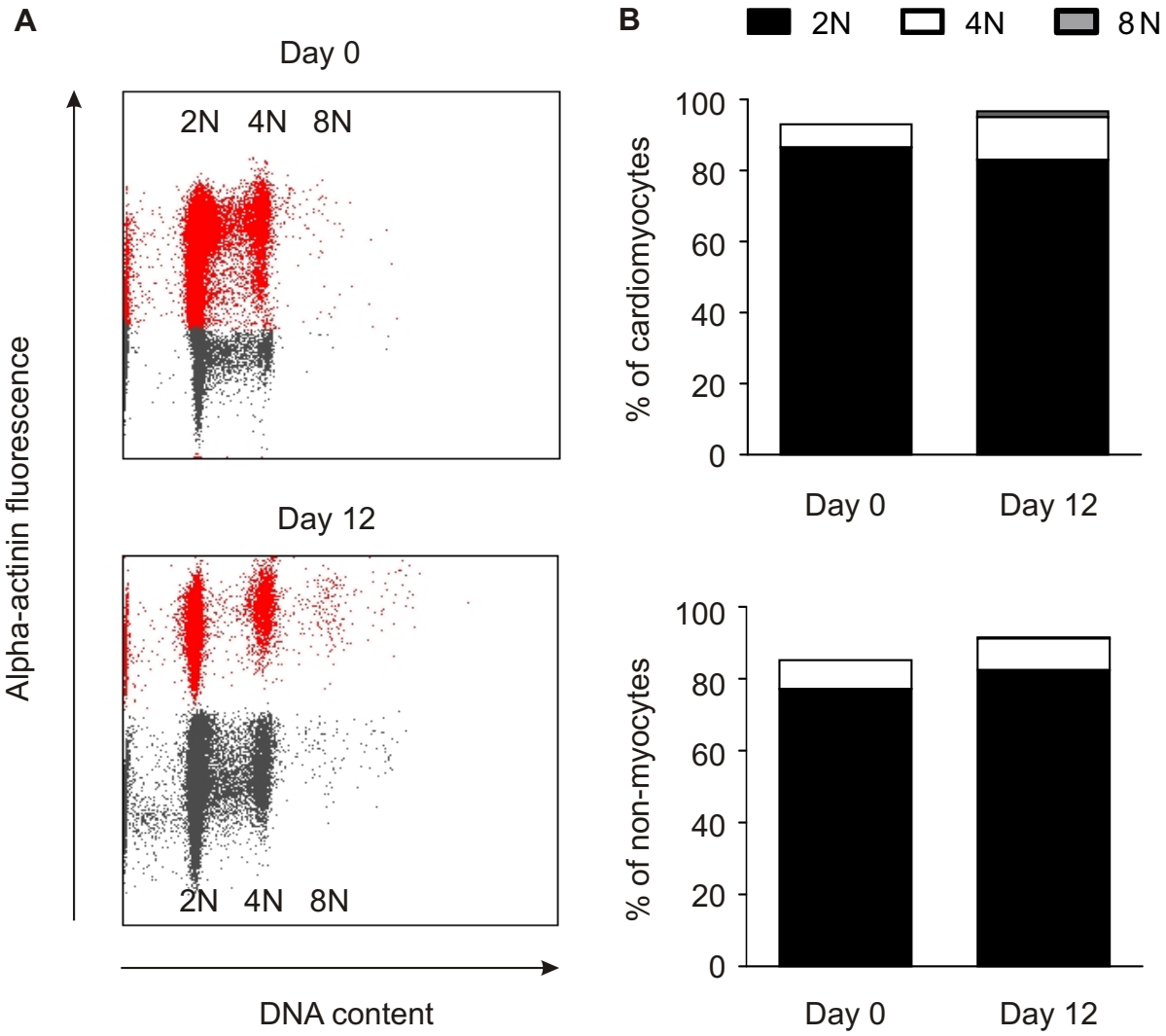

Online Figure II. DNA content in mononucleated cardiomyocytes and fibroblasts during EHT culture assessed by FACS. A, Representative plots of DNA content in mononucleated cardiomyocytes (actinin-positive, red) and non-myocytes (actinin-negative, dark grey) at day 0 and day 12 of EHT culture. **B**, Fractions of mononucleated cardiomyocyte (top panel) and non-myocyte (lower panel) populations at day 0 (n=6) and day 12 (n=4) of EHT culture with 2N, 4N, and 8N DNA content.

Online Figure III

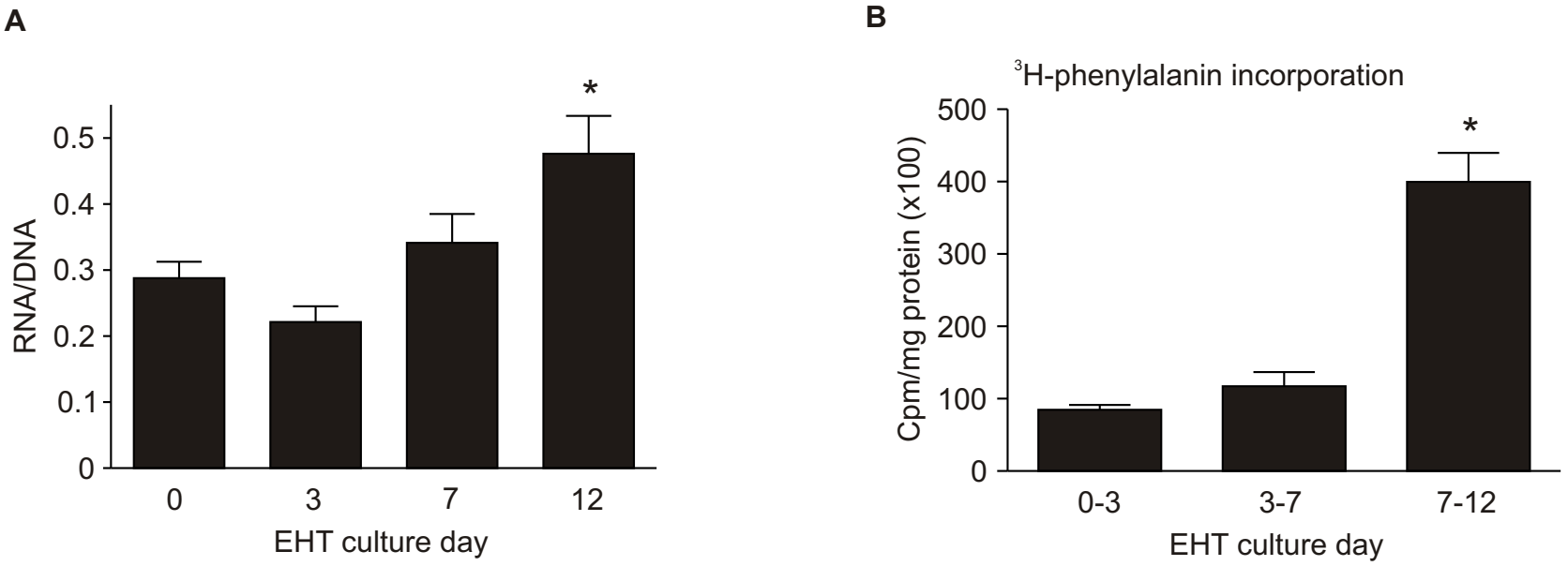

Online Figure III. **Surrogate parameters suggesting hypertrophic growth in EHTs.** **A**, RNA/DNA ratio in EHTs on culture days 0 (n=18), 3 (n=19), 7 (n=10), and 12 (n=16). **B**, ^{3}H-phenylalanine incorporation during EHT culture days 0-3 (n=7), 3-7 (n=8), and 7-12 (n=5). *P< 0.05 vs. EHT day 0 (**A**) and EHT days 0-3 (**B**); ANOVA and Bonferroni's multiple comparison test.

Online Figure IV

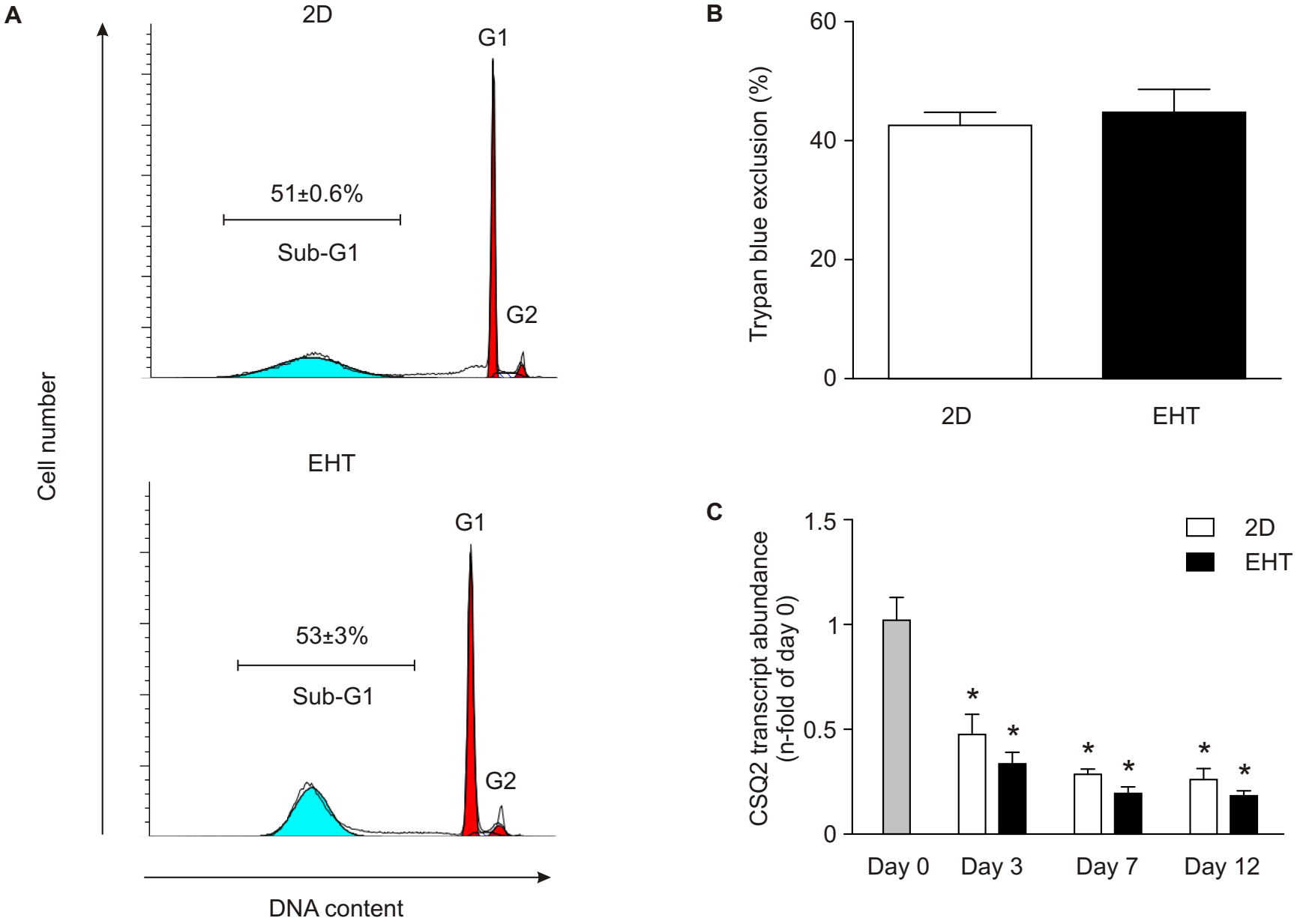

Online Figure IV. **Cell death in EHT and monolayer (2D) culture.** **A**, Analysis of DNA content in EHT- and 2D culture-derived cells (n=3 each). Sub-G1 fraction (green) denotes dead/apoptotic cells with condensed nuclei. **B**, Trypan-blue exclusion in EHT- and 2D culture-derived cells at culture day 1 (n=5 [EHT], n=4 [2D]). **C**, Comparison of CSQ2 transcript abundance in EHT (black bars) vs. 2D culture (white bars), n=5-6/time-point. *P<0.05 vs. day 0 (grey bar); ANOVA and Bonferroni's multiple comparison test.

Online Figure V

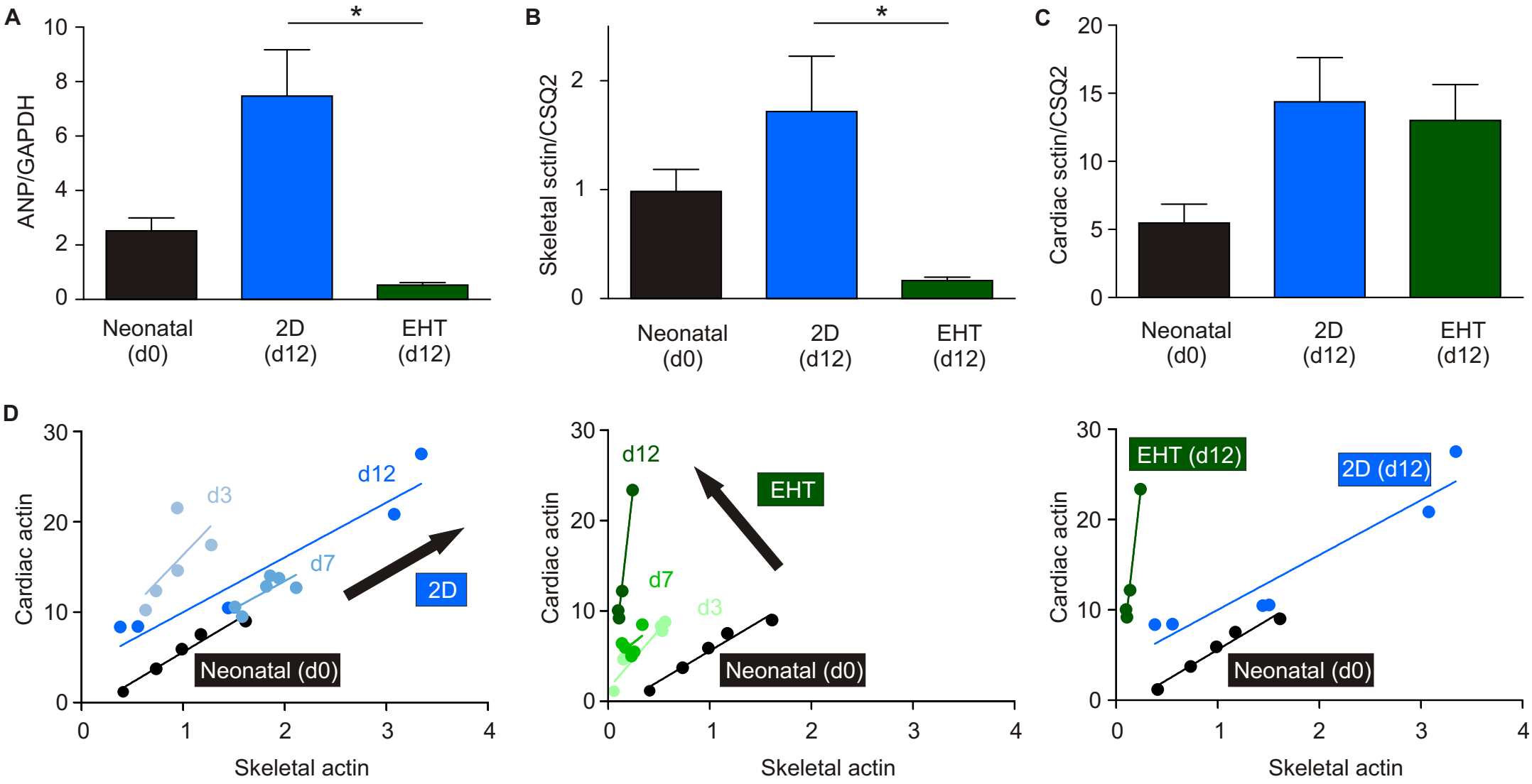

Online Figure V. Molecular markers of maturation in 2D vs. EHT culture. **A**, ANP transcripts per GAPDH transcript; **B**, skeletal actin transcripts per GAPDH transcript; **C**, cardiac actin transcripts per GAPDH transcript in isolated neonatal heart cells at day 0 (black bars; n=5), 2D cultured cells at day 12 (blue bars; n=6), and EHT at day 12 (green bars; n=5). **D**, Correlation of cardiac and skeletal actin transcript abundance in freshly isolated neonatal heart cells (d0; black), in 2D culture (culture days 3,7, and 12 [left panel]) and EHT culture (culture days 3, 7, and 12 [middle panel]) - black arrows denote the trend in expression pattern change in 2D and EHT culture; right panel: direct comparison of 12 day 2D vs. EHT cultures and neonatal cardiomyocytes. *P<0.05 2D vs. EHT; Student's t-test..

Online Figure VI

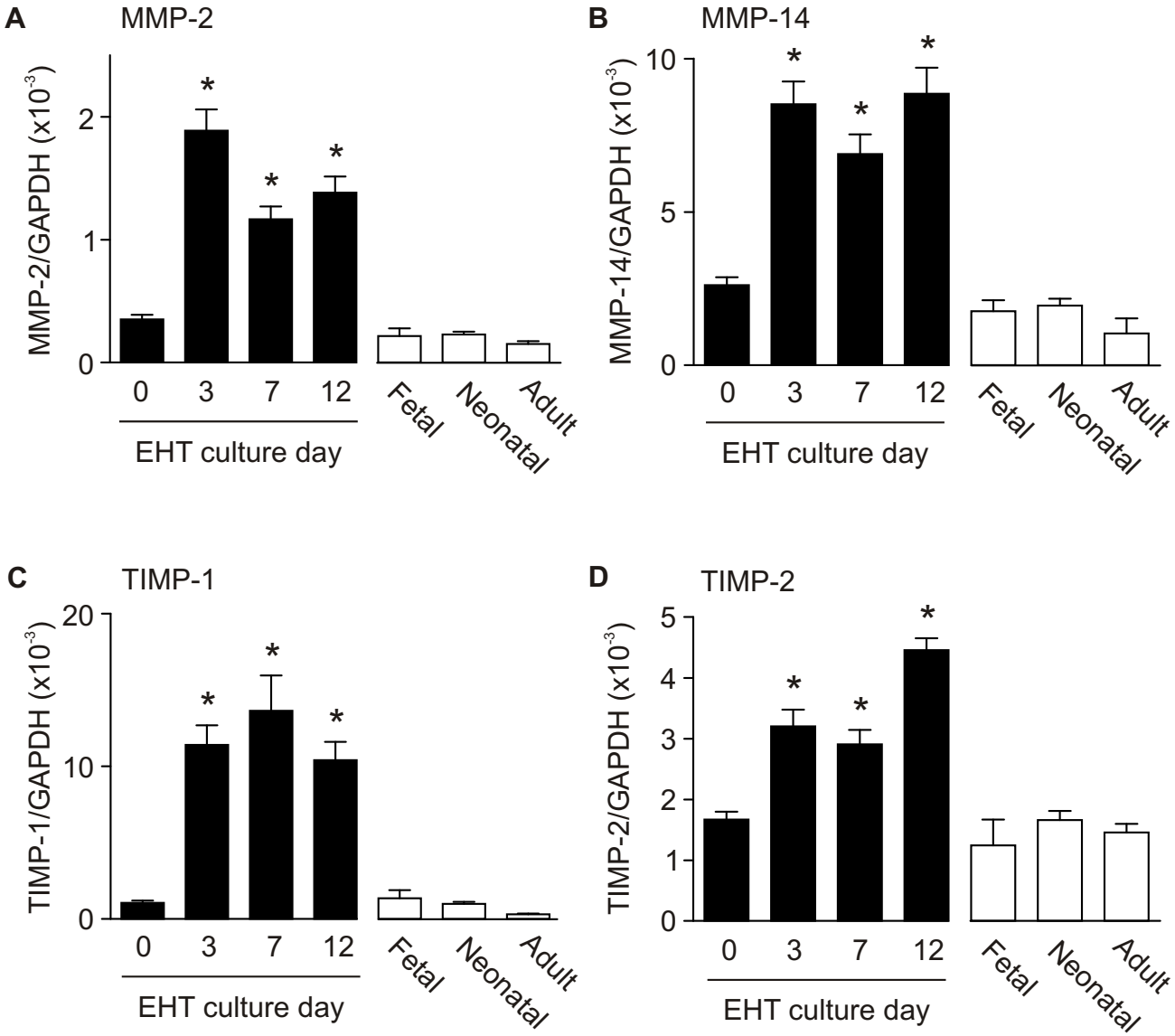

Online Figure VI. ECM restructuring during EHT-development. **A**, matrix metalloprotease-2 (MMP-2; n=8-10); **B**, MMP-14 (n=7-10); tissue inhibitor of matrix metalloprotease-1 (**C**, TIMP-1; n=7-10), and TIMP-2 (**D**; n=7-10) transcripts per GAPDH transcript in EHT and native rat heart tissue. **P*<0.05 vs. EHT day 0; ANOVA followed by Bonferroni's multiple comparison test.

Online Figure VII

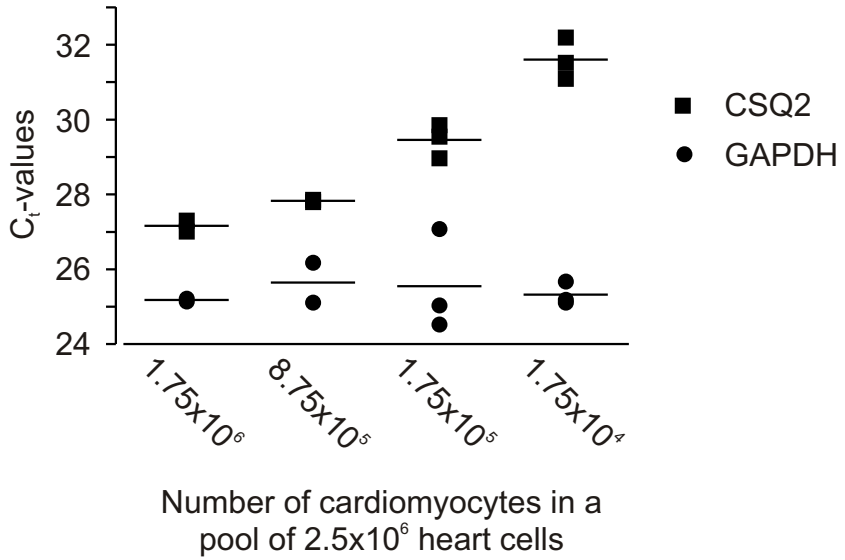

Online Figure VII. Development of a cardiomyocyte-specific qPCR assay to allow approximation of cardiomyocyte content in mixed cell populations. Detection of CSQ2 (NCBI accession#: AF001334; squares) and GAPDH (NCBI accession#: NC005103; circles) transcripts in $2.5x10^6$ cells containing the indicated cardiomyocyte fraction by qPCR. High Ct-values indicate low transcript abundance. Symbols indicate individual Ct-values. Bars indicate the respective means. A Ct-value difference of 3.3 ideally represents a 10-fold difference in transcript abundance. Similar data could be obtained using alternative primer-probe pairs for muscle specific CSQ2 (Ensemble accession#: ENSRNOG00000016243) or 18S-RNA (NCBI accession#: V01270).